Fundamentals of Particle Detectors and Developments in Detector Technologies for Future Experiments

Werner Riegler, CERN

Lecture 6/5

Abstract:

This lecture series will first review the elementary processes and techniques on which particle detectors are based. These must always be kept in mind when discussing the limits of existing technologies and motivations for novel developments. Using the examples of LHC detectors, the limits of state of the art detectors will be outlined and the current detector R&D trends for the LHC upgrade and other future experiments will be discussed. This discussion will include micro-pattern gas detectors, novel solid state detector technologies and trends in microelectronics.

Outline

1) History of Instrumentation

Cloud Chambers/Bubble Chambers/Geiger Counters/Scintillators/Electronics/Wire Chambers

2) Electro-Magnetic Interaction of Charged Particles with Matter

Excitation/ Ionization/ Bethe Bloch Formula/ Range of Particles/ PAI model/ Ionization Fluctuation/ Bremsstrahlung/ Pair Production/ Showers/ Multiple Scattering

3) Signals/Gas Detectors

Detector Signals/ Signal Theorems/
Gaseous Detectors/ Wire Chambers/ Drift Chamber/ TPCs/ RPCs/ Limits of Gaseous Detectors/ Current Trends in Gaseous Detector Development

4) Solid State Detectors

Principles of Solid State Detectors/ Diamond Detectors/ Silicon Detectors/ Limits of Solid State Detectors/ Current Trends in Solid State Detectors

5) Calorimetry & Selected Topics

EM showers/ Hadronic Showers/ Crystal Calorimeters/ Noble Liquid Calirimeters/ Current Trends in Calorimetry

Calorimetry in Particle Physics

This lecture draws heavily from the Review Article

‘Calorimetry for Particle Physics’,
C.W. Fabjan and F. Gianotti, Rev. Mod. Phys., Vol. 75, N0. 4, October 2003

Much information was also taken from the massive Monograph

‘Calorimetry, Energy Measurement in Particle Physics’,
R. Wigmans, Oxford University Press, 2000

Bremsstrahlung

A charged particle of mass M and charge $q=Z_1e$ is deflected by a nucleus of charge Ze which is partially 'shielded' by the electrons. During this deflection the charge is 'accelerated' and it therefore radiated → Bremsstrahlung.

From Bethe's theory we have seen that the elastic scattering off the Nucleus is given by

$$\epsilon_0(q) = Z_2 - \sum_{j=1}^{Z_2} \int e^{i(\vec{q}\vec{r}_j)} \psi_0^2(\vec{r}_j) d^3r_1 ... d^3r_{Z_2} = Z_2 - F \qquad \frac{d\sigma}{d\Omega} = \left(\frac{1}{4\pi\varepsilon_0} \frac{Z_1(Z_2 - F)e_0^2}{2pv} \right)^2 \frac{1}{\sin^4 \theta/2}$$

Where F(q) describes the partial shielding of the nucleus by the electrons. Effective values for F are used in the following expressions.

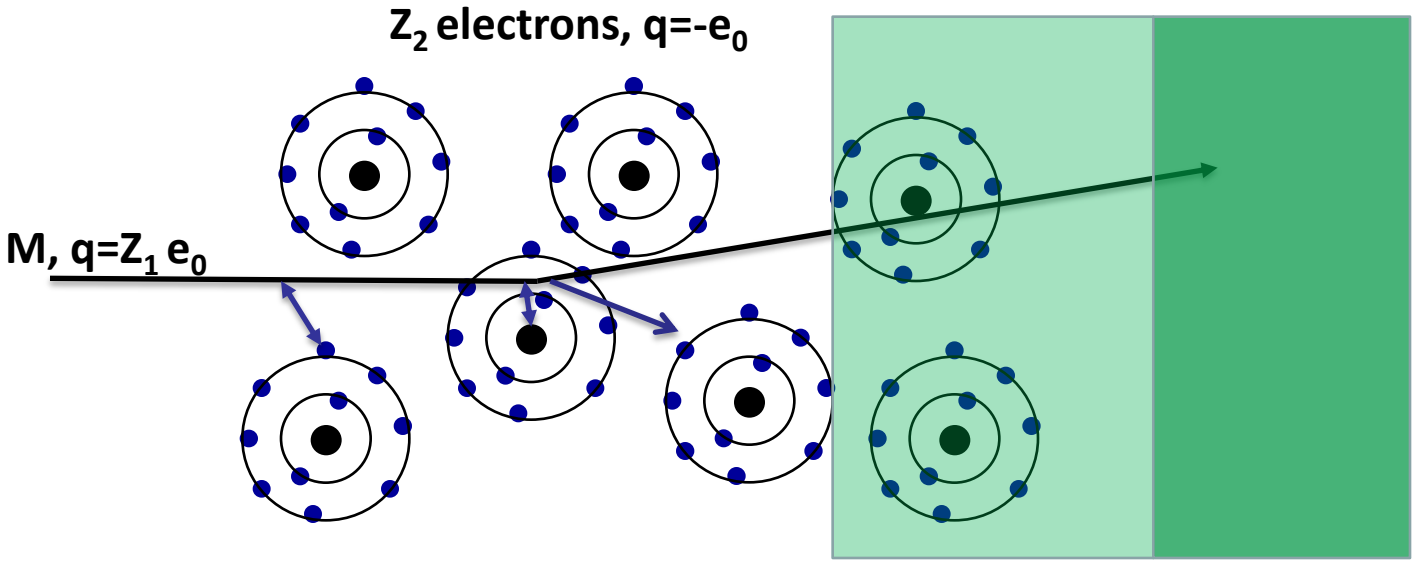

Bremsstrahlung, Classical

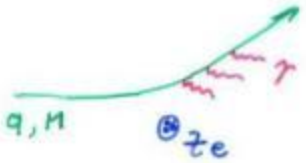

$q = z_1 \cdot e$

$$\frac{d\sigma}{d\Omega} = \left(\frac{2 z_1 z_2 e^2}{4\pi\varepsilon_0 p \cdot v}\right)^2 \frac{1}{(2\sin\frac{\theta}{2})^4} \qquad p = Mv\gamma$$

"Rutherford Scattering"

Written in Terms of Momentum Transfer $Q^2 = 2p^2(1-\cos\theta)$

$$\frac{d\sigma}{dQ} = 8\pi \left(\frac{z_1 z_2 e^2}{4\pi\varepsilon_0 \beta c}\right)^2 \cdot \frac{1}{Q^3}$$

$Q = |\vec{p} - \vec{p}'|$

→ From Maxwell's Eq (Jackson)

$$\lim_{\omega \to 0} \frac{dI}{d\omega} \sim \frac{2}{3\pi} \frac{z_1^2 e^2}{M^2 c^3} \frac{1}{4\pi\varepsilon_0} Q^2$$, Radiated Energy between $\omega, \omega + d\omega$

$$\frac{dE}{dx} = \frac{N_A \varrho}{A} \cdot \int_0^{\omega_{max}} d\omega \int_{Q_{min}}^{Q_{max}} dQ \frac{dI}{d\omega} \cdot \frac{d\sigma}{dQ} \qquad , \omega_{max} = \frac{E}{\hbar}$$

$$\frac{dE}{dx} = \frac{N_A \varrho}{A} \cdot \frac{16}{3} \alpha \cdot z^2 \cdot \left(\frac{z_1 e^2}{4\pi\varepsilon_0 Mc^2}\right)^2 \cdot E \cdot \ln \frac{Q_{max}}{Q_{min}}$$

$$\alpha = \frac{e^2}{4\pi\varepsilon_0 \hbar c} \sim \frac{1}{137}$$

A charged particle of mass M and charge $q=Z_1e$ is deflected by a nucleus of Charge Ze.

Because of the acceleration the particle radiated EM waves → energy loss.

Coulomb-Scattering (Rutherford Scattering) describes the deflection of the particle.

Maxwell's Equations describe the radiated energy for a given momentum transfer.

→ dE/dx

Bremsstrahlung, QM

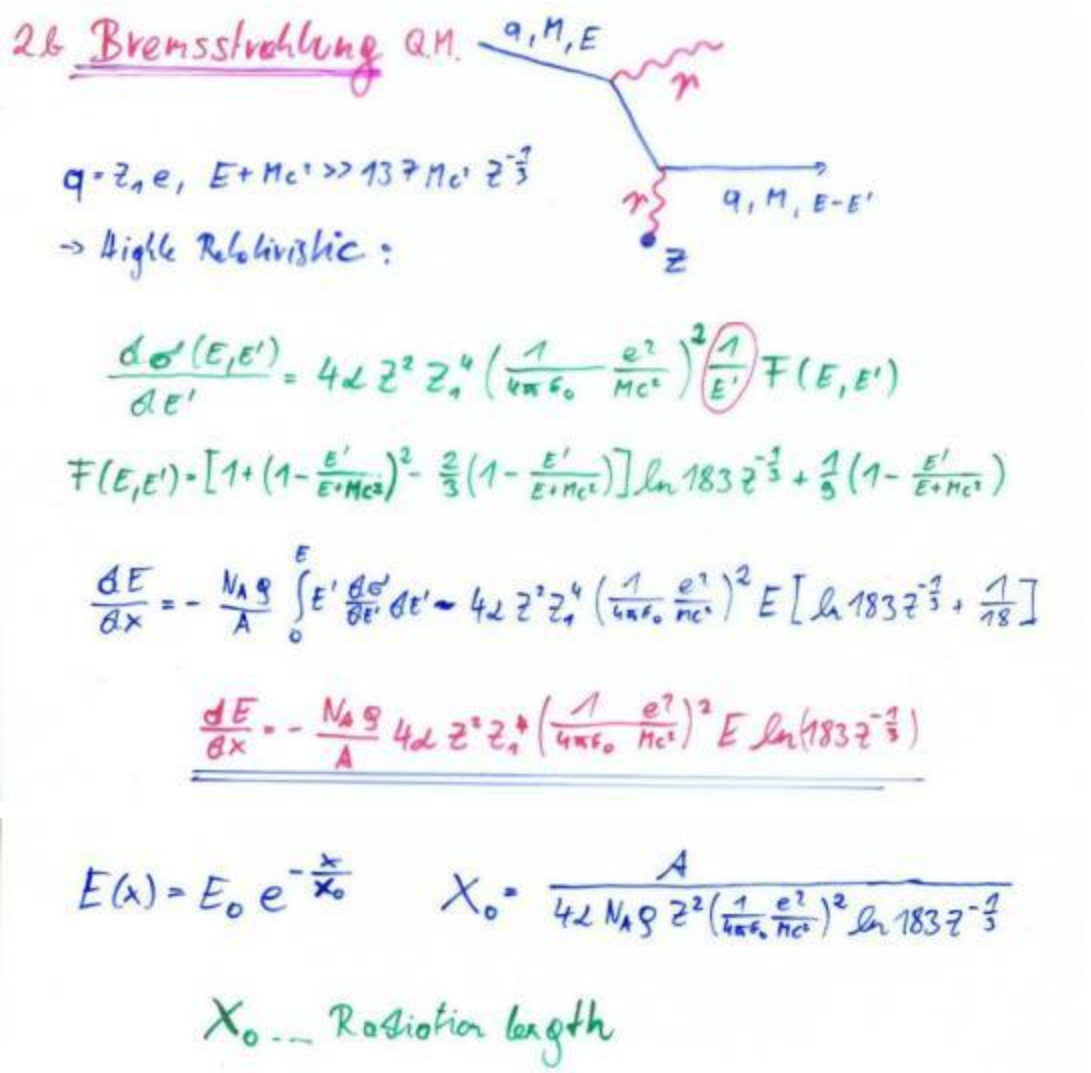

Proportional to Z^2/A of the Material.

Proportional to Z_1^4 of the incoming particle.

Proportional to ρ of the material.

Proportional $1/M^2$ of the incoming particle.

Proportional to the Energy of the Incoming particle →

$E(x)=Exp(-x/X_0)$ – 'Radiation Length'

$X_0 \propto M^2A/ (\rho Z_1^4 Z^2)$

X_0: Distance where the Energy E_0 of the incoming particle decreases $E_0Exp(-1)=0.37E_0$.

Critical Energy

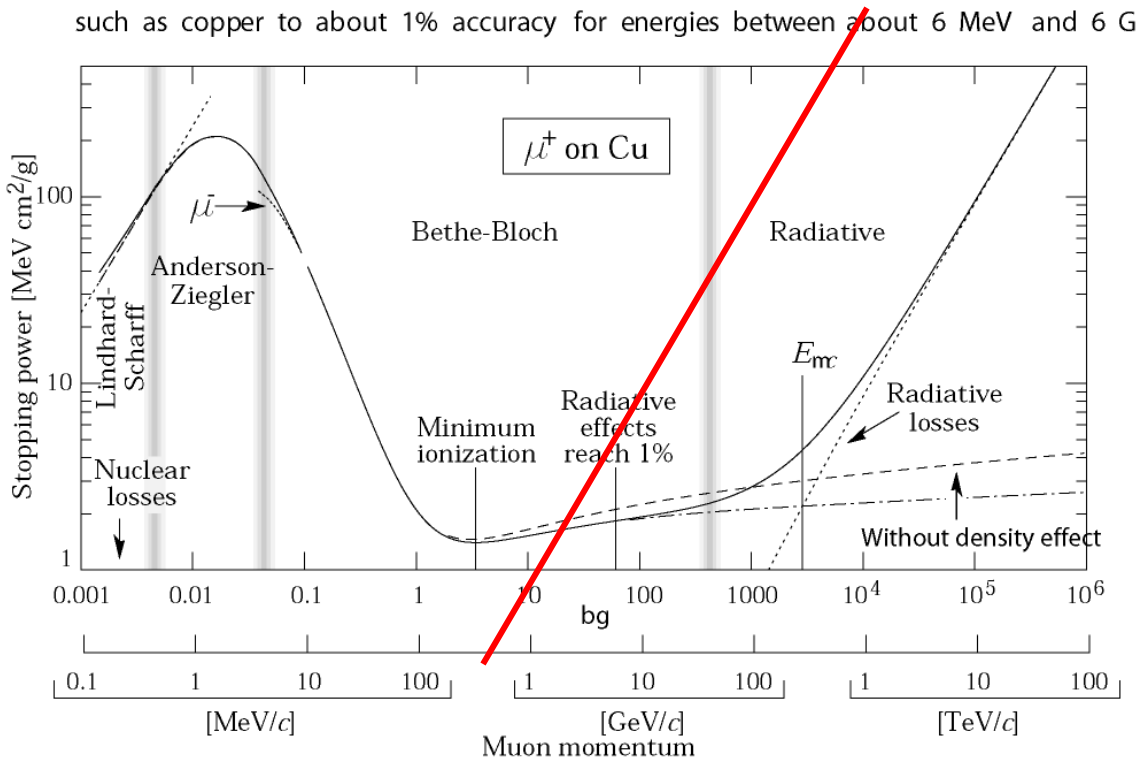

Electron Momentum 5 50 500 MeV/c

For the muon, the second lightest particle after the electron, the critical energy is at 400GeV.

The EM Bremsstrahlung is therefore only relevant for electrons at energies of past and present detectors.

Critical Energy: If dE/dx (Ionization) = dE/dx (Bremsstrahlung)

Myon in Copper: p ≈ 400GeV
Electron in Copper: p ≈ 20MeV

Pair Production, QM

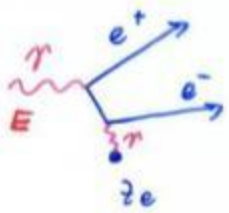

$\gamma + \text{Nucl.} \rightarrow e^+ + e^- + \text{Nucl}$

The Diagram is very similar to Bremsstrahlung

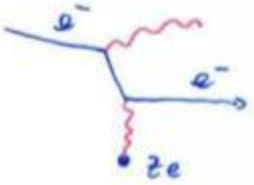

$e^- + \text{Nucl} \rightarrow \gamma + e^- + \text{Nucl}$

"Crossing Symetry: bring particle to the other side and make it the anti particle" -> "same" Correction ...

$$\frac{d\sigma(E,E')}{dE'} = 4\alpha Z^2 r_e^2 \frac{1}{E} \cdot G(E,E') \qquad E \gg 137 m_e c^2 Z^{-\frac{1}{3}}$$

$$G(E,E') = \left[\left(\frac{E'+m_e c^2}{E}\right)^2 \left(1-\frac{E'+m_e c^2}{E}\right)^2 + \frac{2}{3}\frac{E'+m_e c^2}{E}\left(1-\frac{E'+m_e c^2}{E}\right)\right] \ln Z^{-\frac{1}{3}} - \frac{1}{9}\frac{E'+m_e c^2}{E}\left(1-\frac{E'+m_e c^2}{E}\right)\Bigg]$$

$$\sigma = \int_0^{E-2m_e c^2} \frac{d\sigma}{dE'} dE' = 4\alpha Z^2 r_e^2 \cdot \frac{7}{9} \ln 183 Z^{-\frac{1}{3}}$$

$$P(x) = \frac{1}{\lambda} e^{-\frac{x}{\lambda}} \qquad \lambda = \frac{A}{9 N_A \sigma} = \frac{9}{7} X_0$$

↳ Probability that Photon converts to $e^+ e^-$ after a distance x.

For $E\gamma >> m_e c^2 = 0.5\text{MeV}$: $\lambda = 9/7 X_0$

Average distance a high energy photon has to travel before it converts into an e^+ e^- pair is equal to 9/7 of the distance that a high energy electron has to travel before reducing it's energy from E_0 to E_0*Exp(-1) by photon radiation.

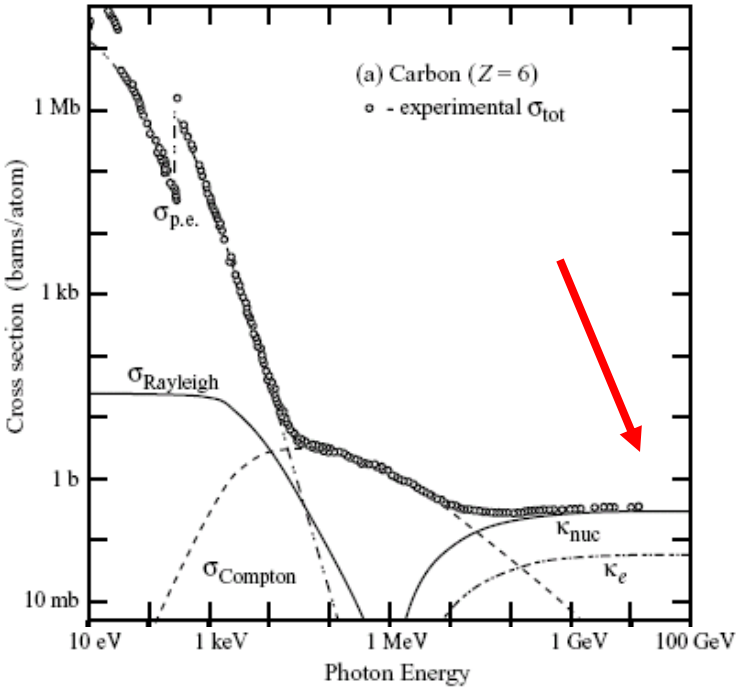

Bremsstrahlung + Pair Production → EM Shower

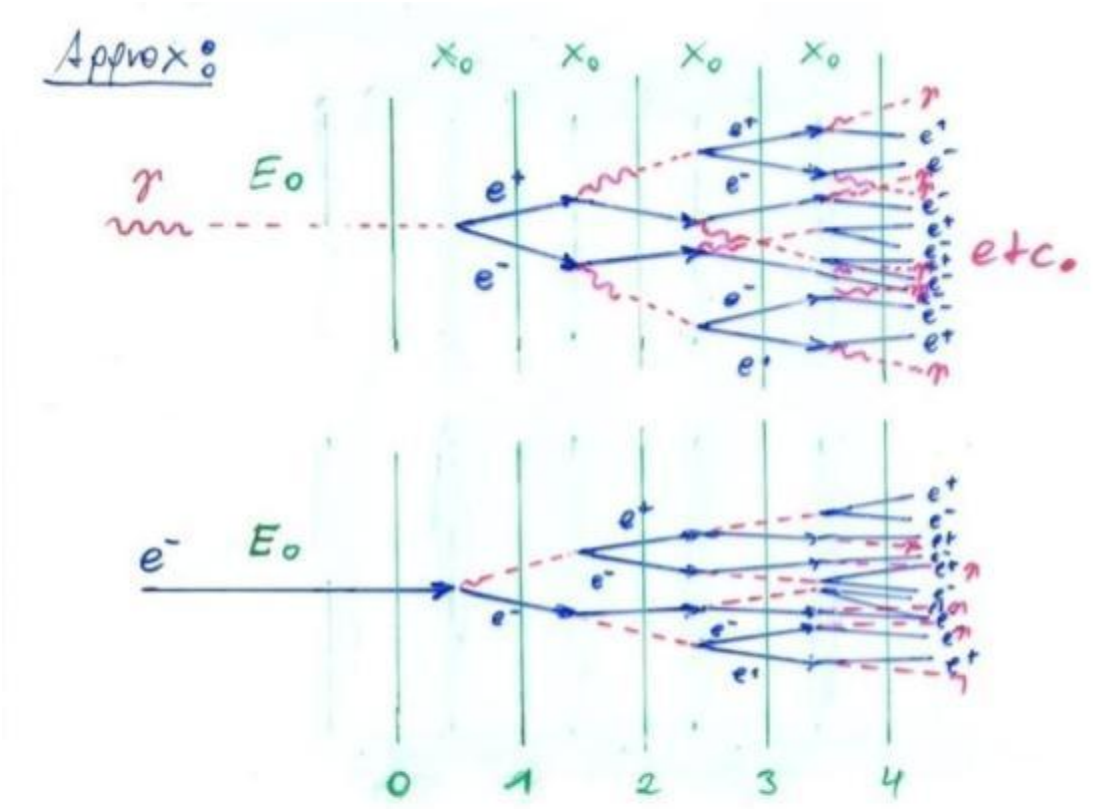

Electromagnetic Shower → EM Calorimeter

Electro-Magnetic Shower of High Energy Electrons and Photons

$N(n) = 2^n$ .... Number of particles ($e^\pm, \gamma$) after $n X_0$

$E(n) = \frac{E_0}{2^n}$ .... Average Energy of particles after $n X_0$

Shower stops if $E(n) = E_{critical}$

$\rightarrow n_{max} = \frac{1}{\ln 2} \ln \frac{E_0}{E_c}$ → Shower length rises with $\ln E_0$

Number of $e^\pm$ track segments (of length X_0) after $n X_0$:

$N_{tr}(n) = 2^n$

Total $e^\pm$ track length (after $n_{max} X_0$)

$$L = \sum_{n=0}^{n_{max}} 2^n X_0 = (2\frac{E_0}{E_c} - 1) X_0 \sim 2\frac{E_0}{E_c} X_0 = c_1 \cdot E_0$$

Total (charged) track length is proportional to the Energy of the Particle.

→ Calorimeter Principle

Calorimetry: Energy Measurement by total Absorption of Particles

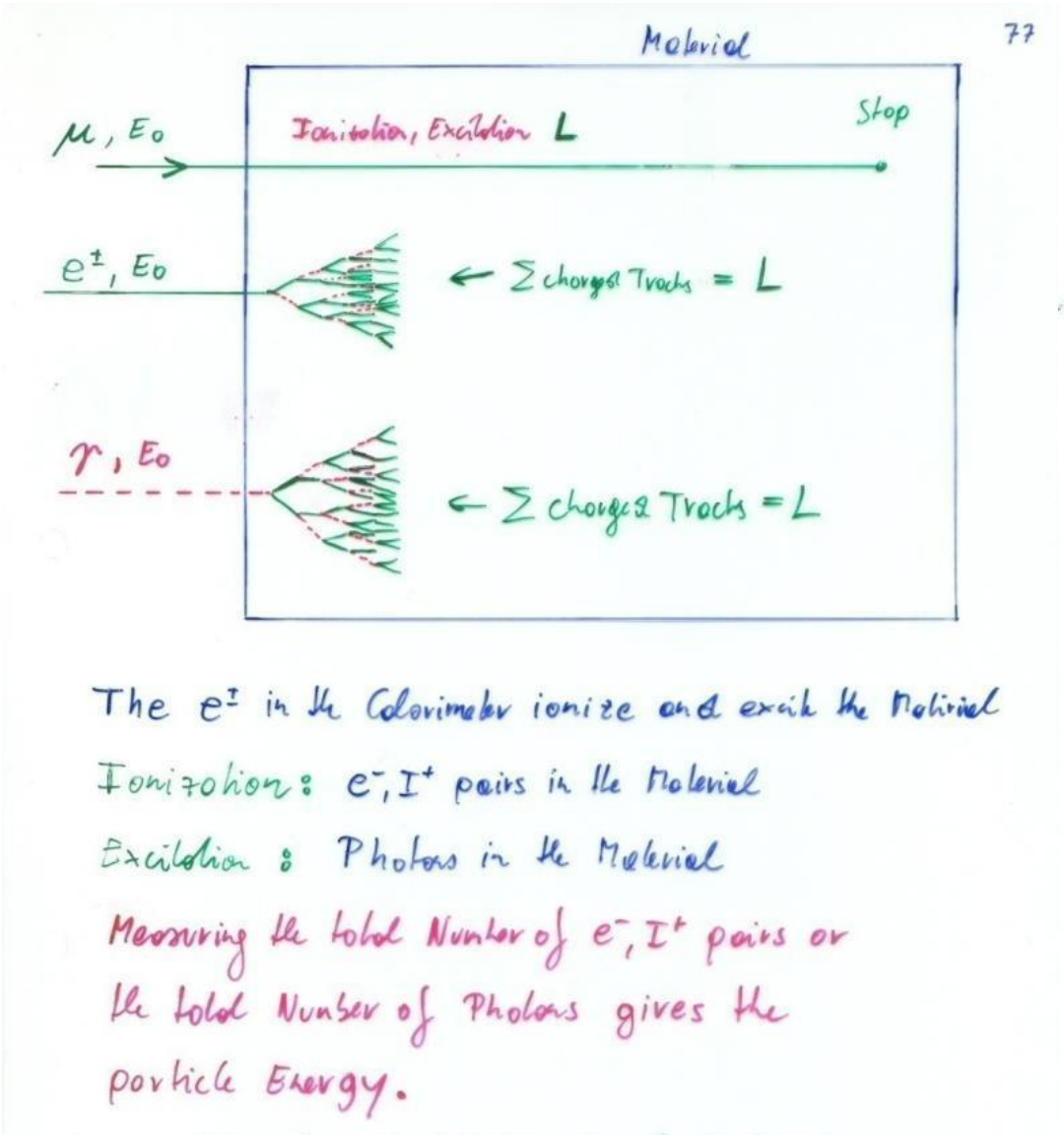

If N is the total Number of e^+, I^+ pairs or photons, or $N = c_1 E_0$:

$\Delta N = \sqrt{N}$ (Poisson Statistics)

$$\frac{\Delta E}{E} = \frac{\Delta N}{N} = \frac{1}{\sqrt{N}} = \frac{a}{\sqrt{E}} \rightarrow \text{Resolution}$$

Only Electrons and High Energy Photons show EM cascades at current GeV-TeV level Energies.

Strongly interacting particles like Pions, Kaons, produce hardonic showers in a similar fashion to the EM cascade →Hadronic calorimetry

Calorimetry: Energy Measurement by total Absorption of Particles

The measurement is destructive. The particle can not be subject to further study.

Energy Measurement by

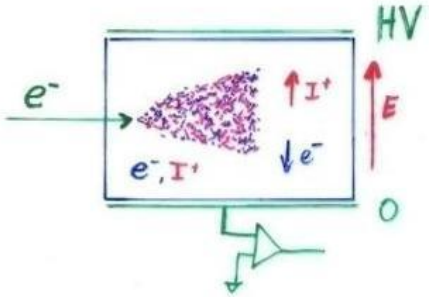

Collecting the produced Charge

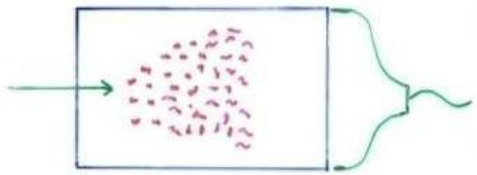

Measuring the Photons produced by the collision of the $e^{\pm}$ with Atom Electrons of the Material.

Total Amount of e^-, I^+ pairs or Photons is proportional to the total track length is proportional to the particle Energy.

Liquid Nobel Gases (Nobel Liquids)

Scintillating Crystals, Plastic Scintillators

Calorimetry

Calorimeters are blocks of instrumented material in which particles to be measured are fully absorbed and their energy transformed into a measurable quantity.

The interaction of the incident particle with the detector (through electro-magnetic or strong processes) produces a shower of secondary particles with progressively degraded energy.

The energy deposited by the charged particles of the shower in the active part of the calorimeter, which can be detected in the form of charge or light, serves as a measurement of the energy of the incident particle.

C.W. Fabjan and F. Gianotti, Rev. Mod. Phys., Vol. 75, N0. 4, October 2003

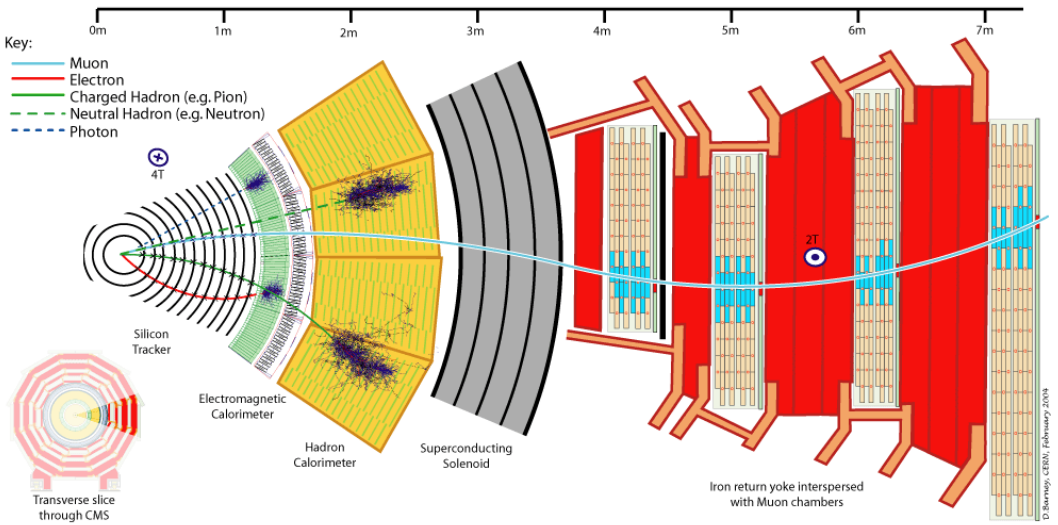

Calorimetry

Calorimeters can be classified into:

Electromagnetic Calorimeters,
to measure electrons and photons through their EM interactions.

Hadron Calorimeters,
Used to measure hadrons through their strong and EM interactions.

The construction can be classified into:

Homogeneous Calorimeters,
that are built of only one type of material that performs both tasks, energy degradation and signal generation.

Sampling Calorimeters,
that consist of alternating layers of an absorber, a dense material used to degrade the energy of the incident particle, and an active medium that provides the detectable signal.

C.W. Fabjan and F. Gianotti, Rev. Mod. Phys., Vol. 75, N0. 4, October 2003

Calorimetry

Calorimeters are attractive in our field for various reasons:

In contrast with magnet spectrometers, in which the momentum resolution deteriorates linearly with the particle momentum, on most cases the calorimeter energy resolution improves as 1/Sqrt(E), where E is the energy of the incident particle. Therefore calorimeters are very well suited for high-energy physics experiments.

In contrast to magnet spectrometers, calorimeters are sensitive to all types of particles, charged and neutral. They can even provide indirect detection of neutrinos and their energy through a measurement of the event missing energy.

Calorimeters are commonly used for trigger purposes since they can provide since they can provide fast signals that are easy to process and interpret.

They are space and therefore cost effective. Because the shower length increases only logarithmically with energy, the detector thickness needs to increase only logarithmically with the energy of the particles. In contrast for a fixed momentum resolution, the bending power BL^2 of a magnetic spectrometer must increase linearly with the particle momentum.

C.W. Fabjan and F. Gianotti, Rev. Mod. Phys., Vol. 75, N0. 4, October 2003

Interaction of Particles with Matter

Any device that is to detect a particle must interact with it in some way → almost …

Neutrinos can be measured by missing transverse energy.

E.g. p p collider E_T=0,
If the Σ E_T of all collision products is ≠0 → neutrino escaped.

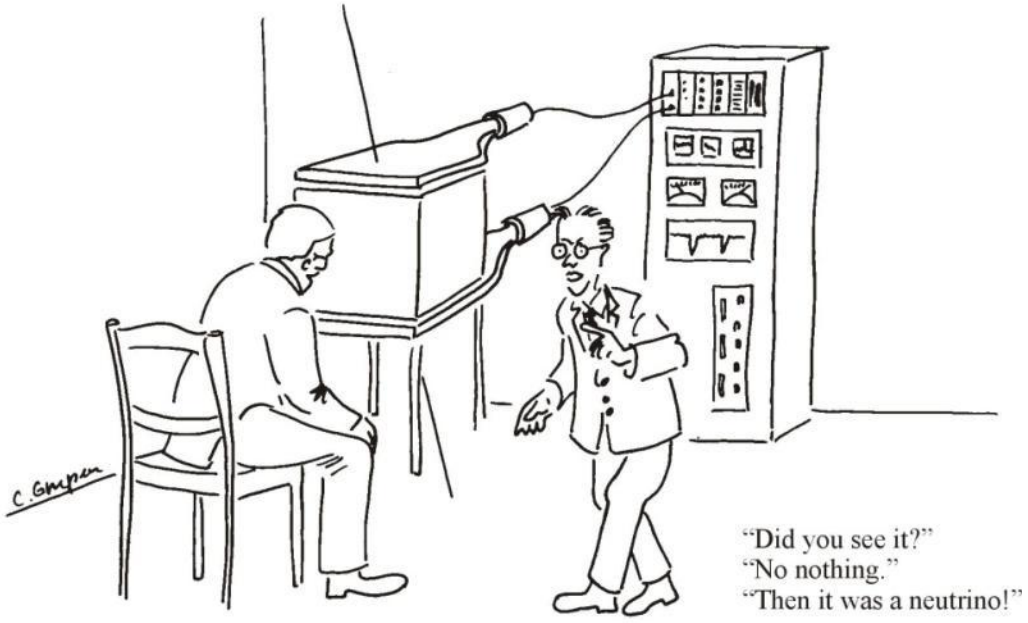

Claus Grupen, Particle Detectors, Cambridge University Press, 1996

EM Calorimetry

Approximate longitudinal shower development

$N(n) = 2^n$ .... Number of particles $(e^{\pm}, \gamma)$ after $n X_0$

$E(n) = \frac{E_0}{2^n}$ .... Average Energy of particles after $n X_0$

Shower stops if $E(n) = E_{critical}$

$\rightarrow n_{max} = \frac{1}{\ln 2} \ln \frac{E_0}{E_c}$ $\rightarrow$ Shower length rises with $\ln E_0$

Radiation Length X_0 and Moliere Radius are two key parameters for choice of calorimeter materials

Approximate transverse shower development

The transverse Shower Dimension is mainly related to the Multiple scattering of the low Energy Electrons.

$$\theta_0 \sim \frac{21\,[\text{MeV}]}{\beta p\,[\frac{\text{MeV}}{c}]} z_1 \cdot \sqrt{\frac{x}{X_0}}$$

Electrons E_c , $E \sim p \cdot c$

$$\theta_0 \sim \frac{21\,[\text{MeV}]}{\beta E_c\,[\text{MeV}]} \cdot z_1 \cdot \sqrt{\frac{x}{X_0}} \qquad z_1 = 1\,,\ \beta \sim 1$$

$$E_c \sim \frac{610}{Z+1.24}\ \text{MeV} \sim \frac{610}{Z}\ \text{MeV}$$

$$\theta_0 = 0.0344 \cdot Z \cdot \sqrt{\frac{x}{X_0}}$$

Moliere Radius ρ_m = lateral Shower Radius after $1 X_0$:

$$\rho_m \approx 0.0344 \cdot Z \cdot X_0$$

95% of Energy are in a Cylinder of $2\rho_m$ Radius.

Simulated EM Shower Profiles in $PbWO_4$

Simulation of longitudinal shower profile **Simulation of transverse shower profile**

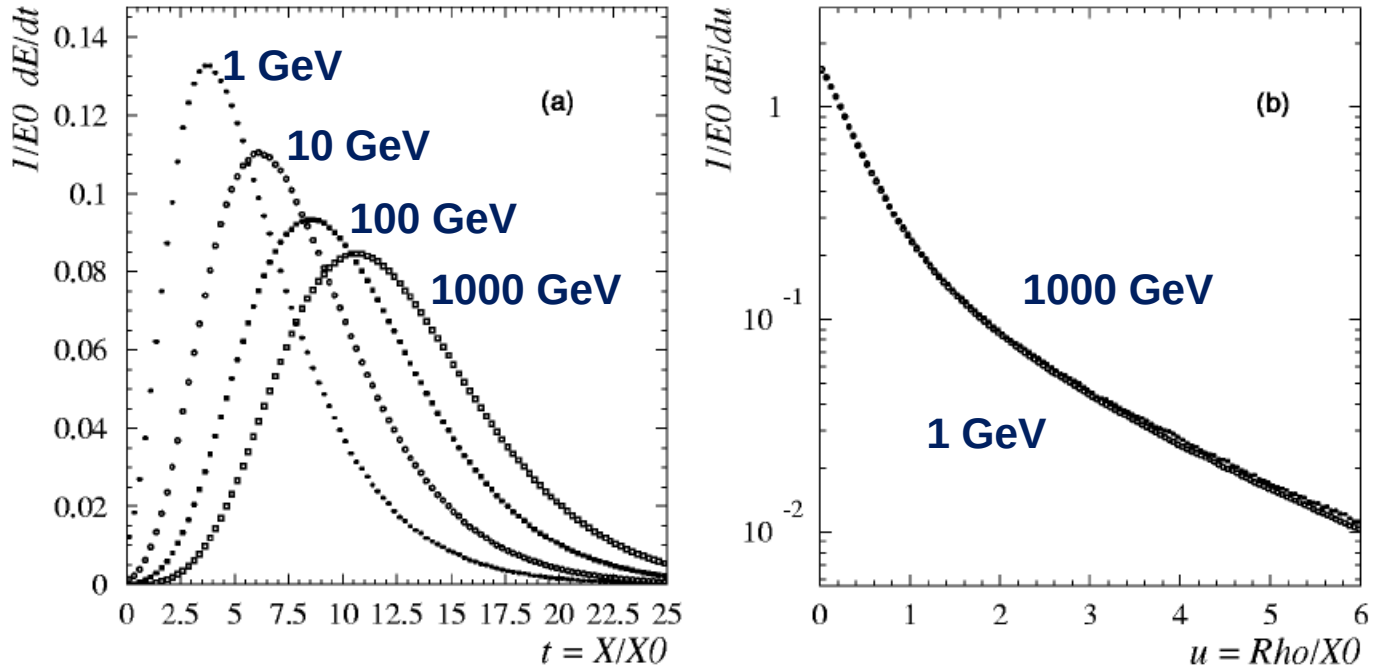

FIG. 2. (a) Simulated shower longitudinal profiles in $PbWO_4$, as a function of the material thickness (expressed in radiation lengths), for incident electrons of energy (from left to right) 1 GeV, 10 GeV, 100 GeV, 1 TeV. (b) Simulated radial shower profiles in $PbWO_4$, as a function of the radial distance from the shower axis (expressed in radiation lengths), for 1 GeV (closed circles) and 1 TeV (open circles) incident electrons. From Maire (2001).

In calorimeters with thickness ~ 25 X_0, the shower leakage beyond the end of the active detector is much less than 1% up to incident electron energies of ~ 300 GeV (LHC energies).

Crystals for Homogeneous EM Calorimetry

In crystals the light emission is related to the crystal structure of the material. Incident charged particles create electron-hole pairs and photons are emitted when electrons return to the valence band.

The incident electron or photon is completely absorbed and the produced amount of light, which is reflected through the transparent crystal, is measured by photomultipliers or solid state photon detectors.

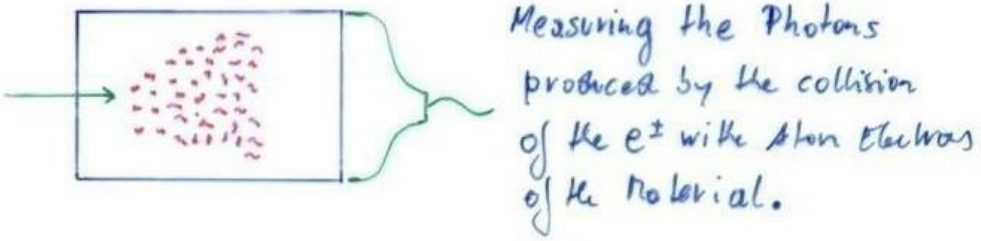

Crystals for Homogeneous EM Calorimetry

	NaI(Tl)	CsI(Tl)	CsI	BGO	$PbWO_4$
Density (g/cm^3)	3.67	4.53	4.53	7.13	8.28
X_0 (cm)	2.59	1.85	1.85	1.12	0.89
R_M (cm)	4.5	3.8	3.8	2.4	2.2
Decay time (ns)	250	1000	10	300	5
slow component			36		15
Emission peak (nm)	410	565	305	410	440
slow component			480		
Light yield γ/MeV	4×10^4	5×10^4	4×10^4	8×10^3	1.5×10^2
Photoelectron yield (relative to NaI)	1	0.4	0.1	0.15	0.01
Rad. hardness (Gy)	1	10	10^3	1	10^5

Barbar@PEPII, 10ms interaction rate, good light yield, good S/N

KTeV@Tevatron, High rate, Good resolution

L3@LEP, 25us bunch crossing, Low radiation dose

CMS@LHC, 25ns bunch crossing, high radiation dose

Crystals for Homogeneous EM Calorimetry

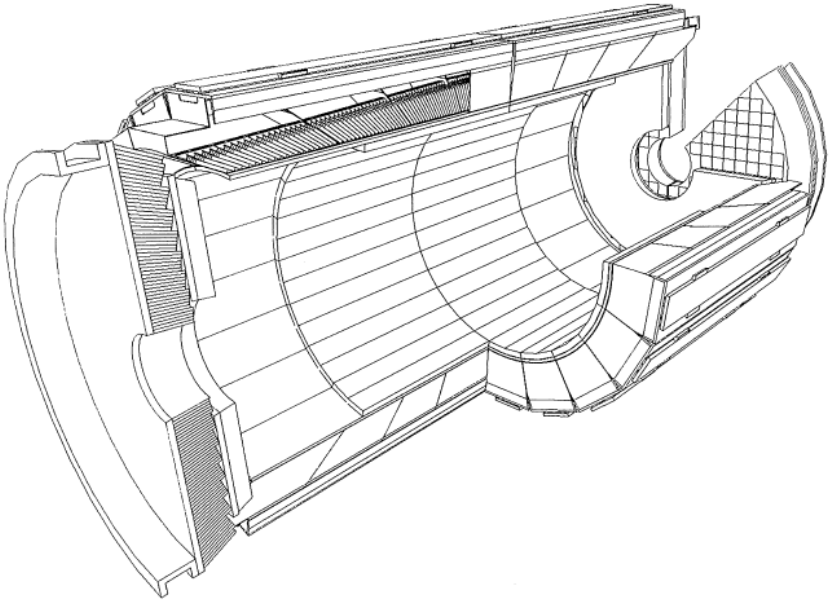

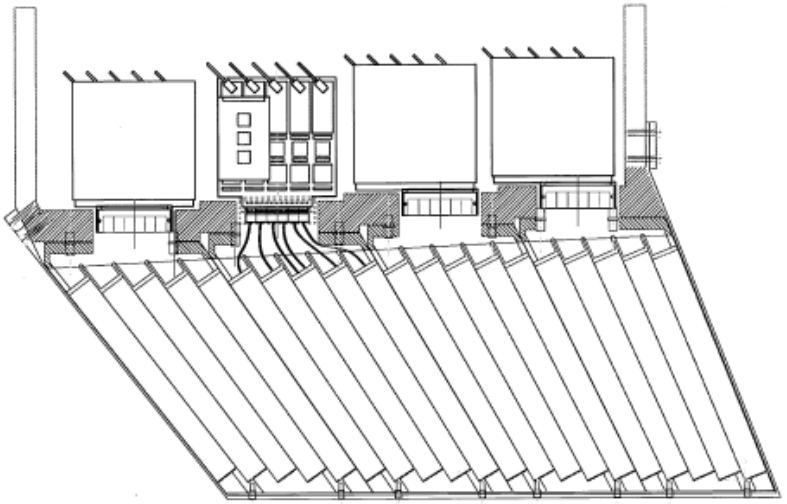

Fig. 2. Longitudinal drawing of module 2, showing the structure and the front-end electronics layout.

Noble Liquids for Homogeneous EM Calorimetry

	Ar	Kr	Xe
Z	18	36	58
A	40	84	131
X_0 (cm)	14	4.7	2.8
R_M (cm)	7.2	4.7	4.2
Density (g/cm^3)	1.4	2.5	3.0
Ionization energy (eV/pair)	23.3	20.5	15.6
Critical energy ϵ (MeV)	41.7	21.5	14.5
Drift velocity at saturation (mm/μs)	10	5	3

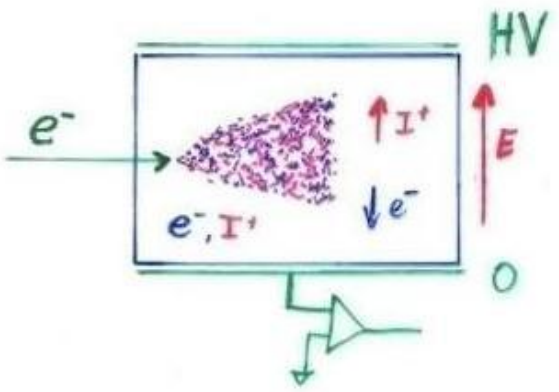

When a charge particle traverses these materials, about half the lost energy is converted into ionization and half into scintillation.

The best energy resolution would obviously be obtained by collecting both the charge and light signal. This is however rarely done because of the technical difficulties to extract light and charge in the same instrument.

Krypton is preferred in homogeneous detectors due to small radiation length and therefore compact detectors. Liquid Argon is frequently used due to low cost and high purity in sampling calorimeters (see later).

Noble Liquids for Homogeneous EM Calorimetry

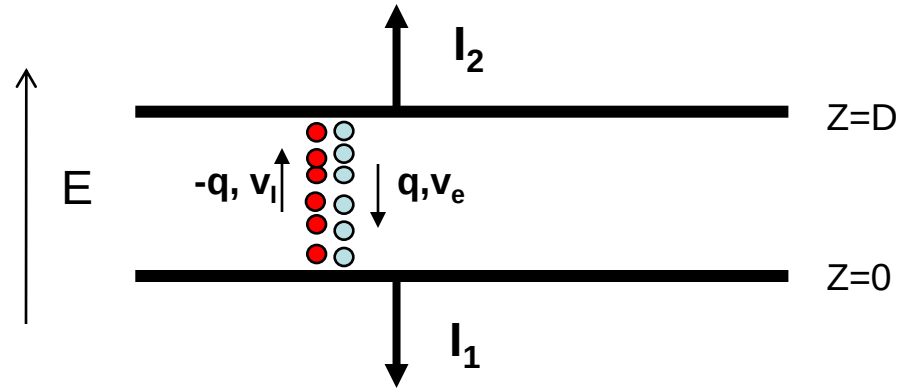

E.g. Liquid Argon, 5mm/ µs at 1kV/cm, 5mm gap → 1 µs for all electrons to reach the electrode.

The ion velocity is 10^3 to 10^5 times smaller → doesn't contribute to the signal for electronics of µs integration time.

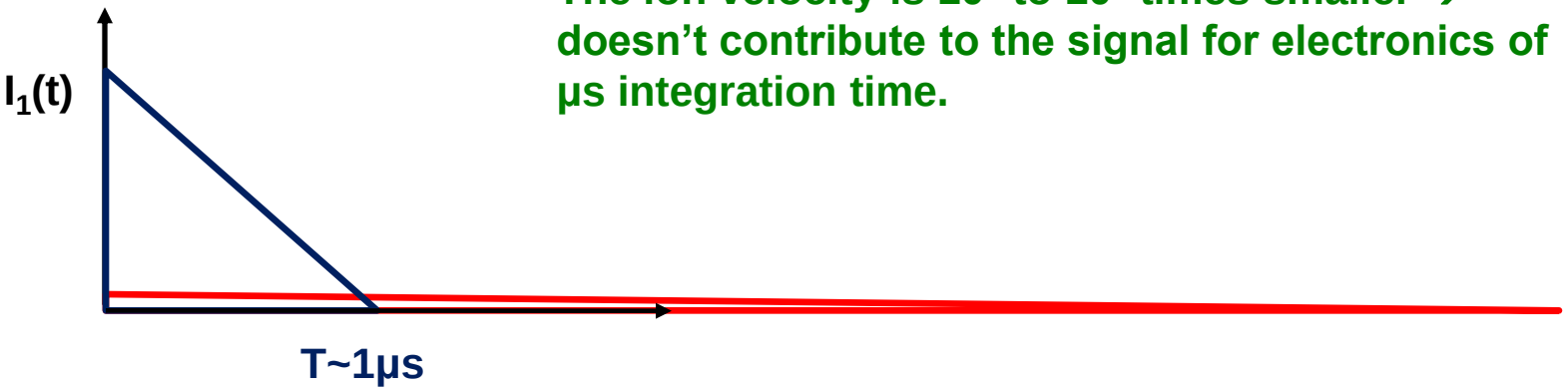

Homogeneous EM Calorimeters, Examples

NA48 Liquid Krypton
2cmx2cm cells
X_0 = 4.7cm
125cm length ($27X_0$)
ρ = 5.5cm

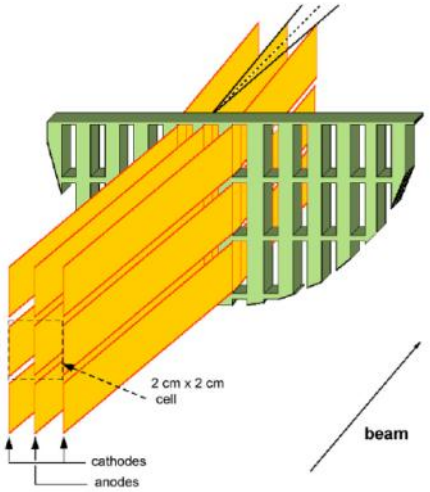

KTeV CsI
5cmx5cm and
X_0 = 1.85cm
2.5cmx2.5cm crystals
50cm length ($27X_0$)
ρ = 3.5cm

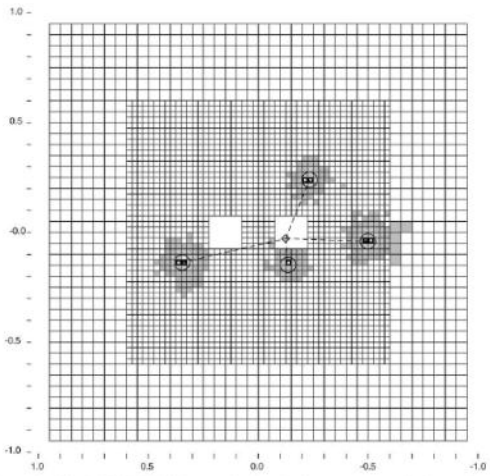

Fig. 1. Schematic of the KTeV CsI Calorimeter showing the cluster energy profiles due to four photons.

NA48 Experiment at CERN and KTeV Experiment at Fermilab, both built for measurement of direct CP violation. Homogenous calorimeters with Liquid Krypton (NA48) and CsI (KTeV). Excellent and very similar resolution.

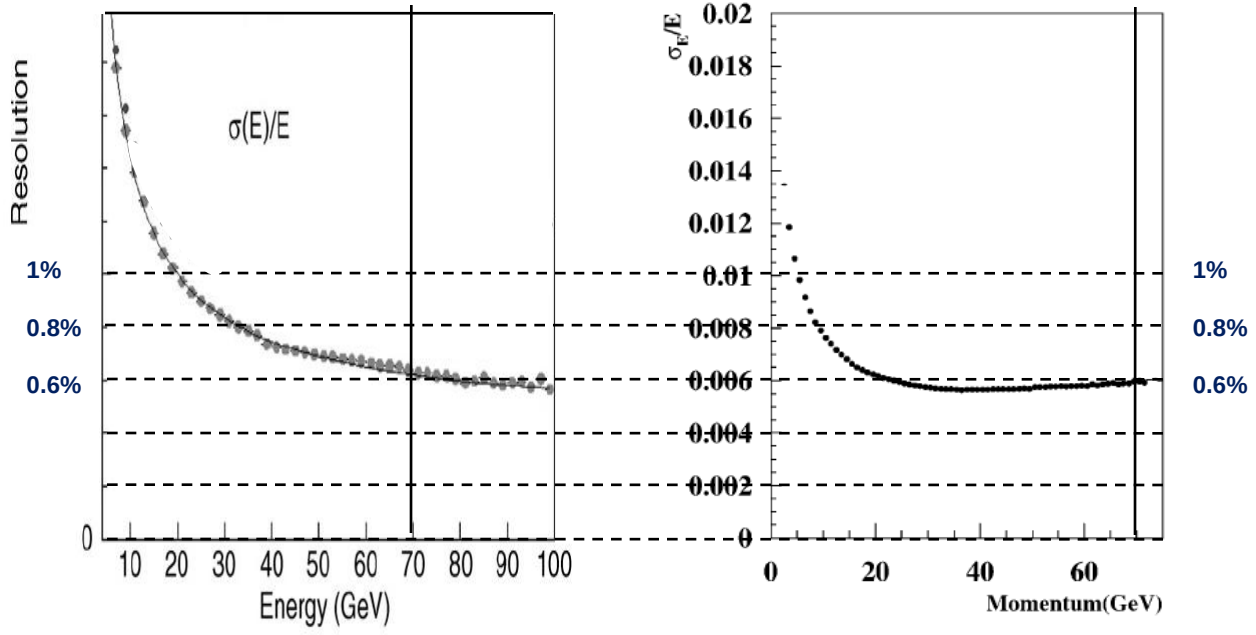

Energy Resolution of Calorimeters

Stochastic term:
Fluctuations related to the physics development of the shower.

Noise term:
From electronics noise of the readout chain.
For constant electronics noise
→ double signal = double S/N

Constant term:
Instrumental effects that cause variations of the calorimeter response with the particle impact point.

$$\frac{\sigma}{E} = \frac{a}{\sqrt{E}} \oplus \frac{b}{E} \oplus c$$

Add in squares

For homogeneous calorimeters the noise term and constant term become dominant.

For sampling calorimeters the stochastic term, then called 'sampling' term becomes dominant.

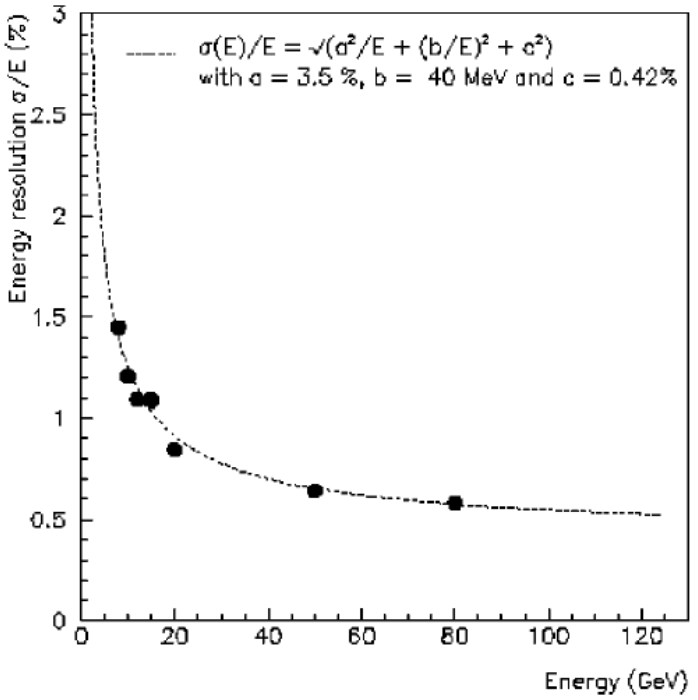

FIG. 3. Fractional electron energy resolution as a function of energy measured with a prototype of the NA48 liquid krypton electromagnetic calorimeter (NA48 Collaboration, 1995). The line is a fit to the experimental points with the form and the parameters indicated in the figure.

Sampling Calorimeters

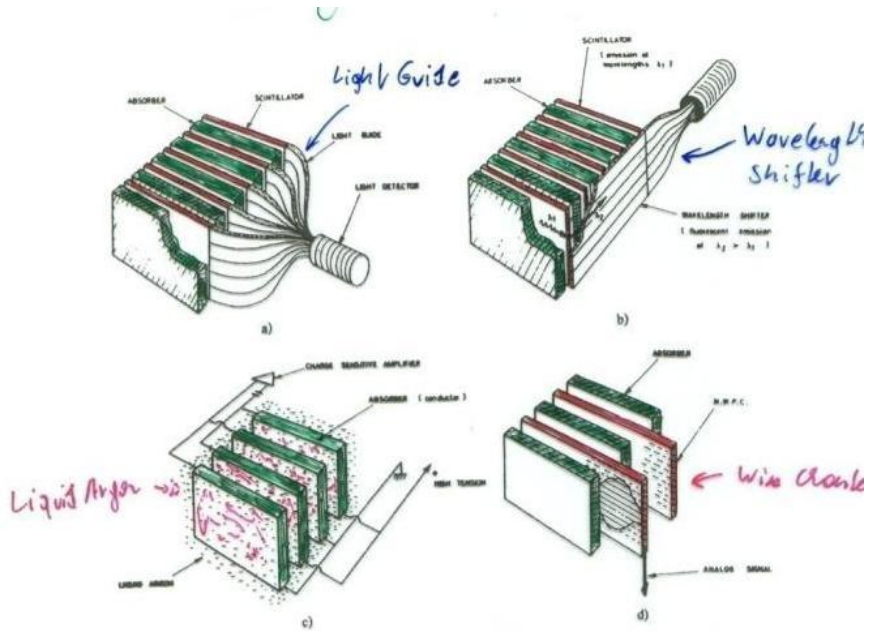

Alternation of "passive" absorber plates and "active" readout sections

Advantage:
- optimum choice of Absorber Material
- optimum choice of Signal Readout
- Compact and cheap Construction

"passive": Pb, Fe ....

"active": Scintillator (Signal → Photons)
Noble Liquid, e.g. Ar (Signal → e^-, I^+)
Wire Chambers (Signal → e^-, I^+)

Energy resolution of sampling calorimeters is in general worse than that of homogeneous calorimeters, owing to the sampling fluctuations – the fluctuation of ratio of energy deposited in the active and passive material.

The resolution is typically in the range 5-20%/Sqrt[E(GeV)] for EM calorimeters. On the other hand they are relatively easy to segment longitudinally and laterally and therefore they usually offer better space resolution and particle identification than homogeneous calorimeters.

The active medium can be scintillators (organic), solid state detectors, gas detectors or liquids.

Sampling Fraction = Energy deposited in Active/Energy deposited in passive material.

Scintillator Sampling Calorimeters

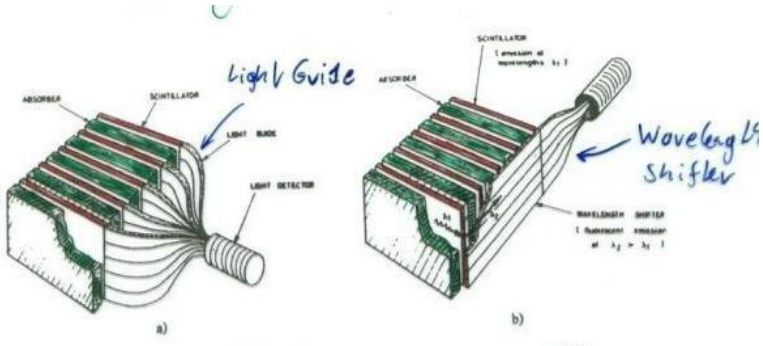

Wavelength shifters absorb photons from the scintillators and emit light at a longer wavelength which does not go back into the scintillator but is internally reflected along the readout plate to the photon detector → compact design.

A large number of sampling calorimeters use organic scintillators arranged in fibers or plates.

The drawbacks are that the optical readout suffers from radiation damage and non-uniformities at various stages are often the source of a large constant term.

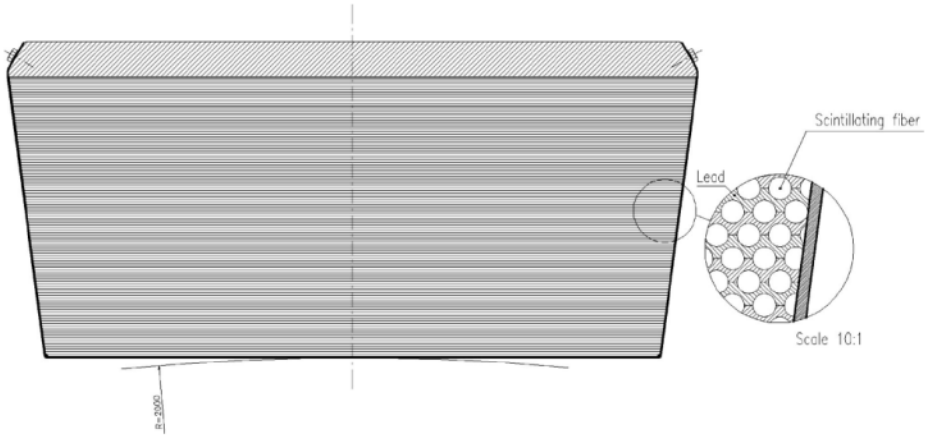

FIG. 13. Schematic layout of the barrel part of the KLOE electromagnetic calorimeter (Antonelli *et al.*, 1995).

Kloe EM calorimeter:

5%/Sqrt[E(GeV)] !

Gas and Solid State Sampling Calorimeters

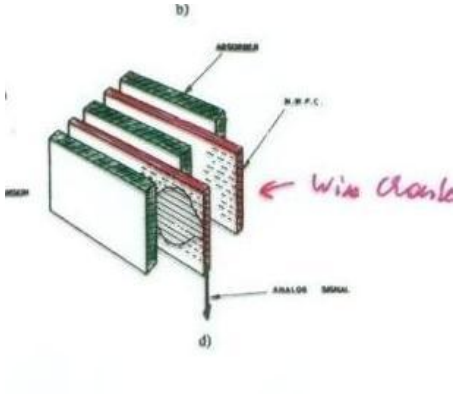

Gas sampling calorimeters have been widely employed until recently (LEP) because of their low cost and segmentation flexibility.

They are not well suited to present and future machines because of their modest EM energy resolution ~ 20%/Sqrt[E(GeV)].

Solid state detectors as active readout medium use mostly silicon. The advantage is very high signal to noise ratio (large signals). Often used on a small scale as luminosity monitors.

The disadvantage is the high cost, preventing large calorimeters, and poor radiation resistance.

Liquid Sampling Calorimeters

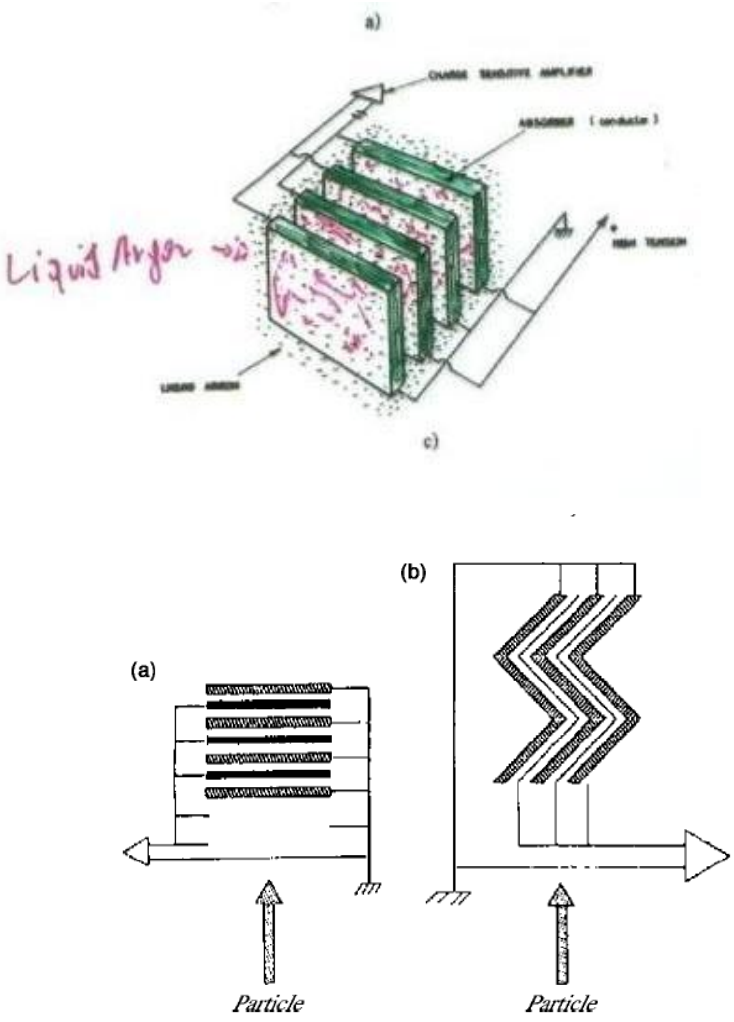

FIG. 15. Schematic view of a traditional sampling calorimeter geometry (a) and of the accordion calorimeter geometry (b).

These offer good application perspectives for future experiments.

Warm liquids work at room temperature, avoiding cryogenics but they are characterized by poor radiation resistance and suffer from purity problems

→Noble liquids at cryogenic temperatures.

The advantages are operation in 'ion chamber mode', i.e. deposited charge is large and doesn't need multiplication, which ensures better uniformity compared to gas calorimeters that need amplification.

They are relatively uniform and easy to calibrate because the active medium is homogeneously distributed inside the volume. They provide good energy resolution (e.g. ATLAS 10%/Sqrt[E(GeV)])
And stable operation with time.

They are radiation hard.

With the standard liquid argon sampling calorimeters the alternating absorber and active layers are disposed perpendicular to the direction of the incident particle.
→ Long cables are needed to gang together the readout electrodes, causing signal degradation, dead spaces between the calorimeter towers and therefore reduced hermeticity.

Liquid Argon Sampling Calorimeters

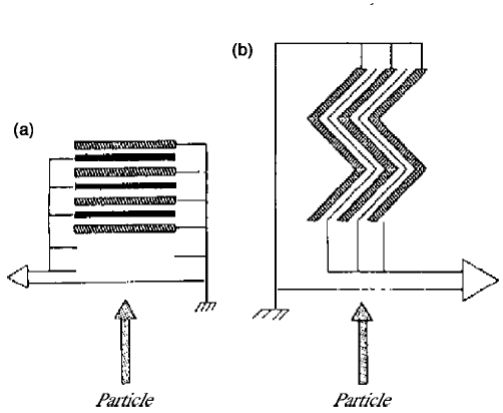

FIG. 15. Schematic view of a traditional sampling calorimeter geometry (a) and of the accordion calorimeter geometry (b).

For the ATLAS LAr Calorimeter this was solved by placing the absorbers in an accordeon geometry parallel to the particle direction and the electrodes can easily be read out from the 'back side'.

ATLAS: Lead layers of 1.1-2.2mm, depending on the rapidity region, are separated by 4mm liquid Argon gaps.

Test beam results show
10%/Sqrt[E(GeV)] x 0.25/E(GeV) x 0.3%

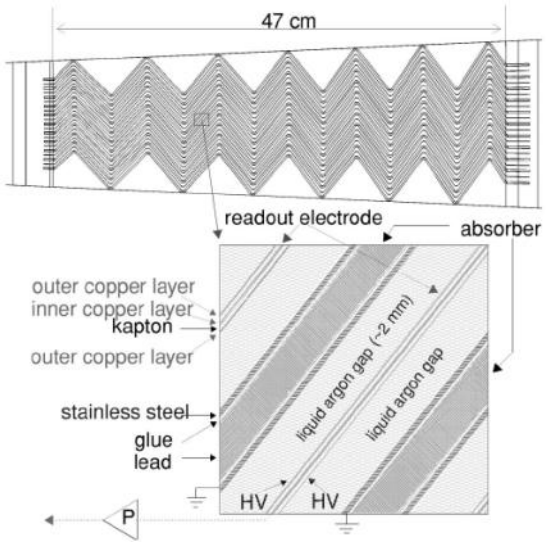

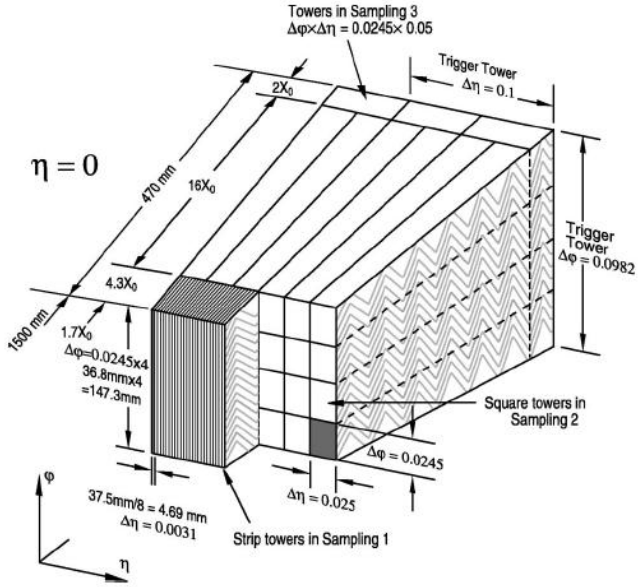

FIG. 17. Schematic view of the segmentation of the ATLAS electromagnetic calorimeter.

Hadronic Calorimetry

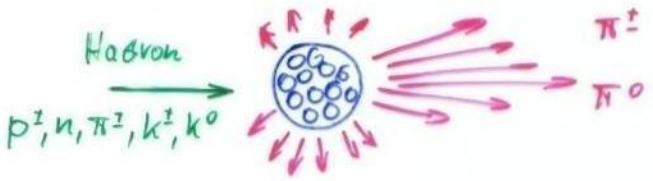

Strong Interaction

Approximate Energy Distribution

~50%	~20%	~30%
π^+, π^- π^0	Nuclear Excitation	Slow Nucleons
$\gamma\gamma$	5-30 MeV	
π^+, π^- $\pi^+\pi^-, \pi^0$	p, n, γ	
$\gamma\gamma$		

Hadron kaskade

$\pi^0 \to \gamma\gamma \to$ Electromagnetic Component

In Hadronic Cascades the Longitudinal Shower is given by the Absorption Length λ_a $\quad I \sim e^{-\frac{x}{\lambda_a}}$

In typical Detector Materials λ_a is much larger than X_0

$$\lambda \sim \frac{1}{\rho} \cdot 35\, A^{\frac{1}{3}}$$

	ρ	X_0	λ
Fe	7.87	1.76 cm	~17 cm
Pb	11.35	0.56 cm	~17 cm

Energy Resolution:

- A large Fraction of the Energy 'disappears' into
  - Binding Energy of emitted Nucleons
  - $\pi \to \mu + \nu$ which are not absorbed
- π^0's Decaying into $\gamma\gamma$ start an EM Cascade ($\tau \sim 10^{-14}$ s)

– Energy Resolution is worse than for EM Calorimeters

Hadron Calorimeters are Large because λ is large

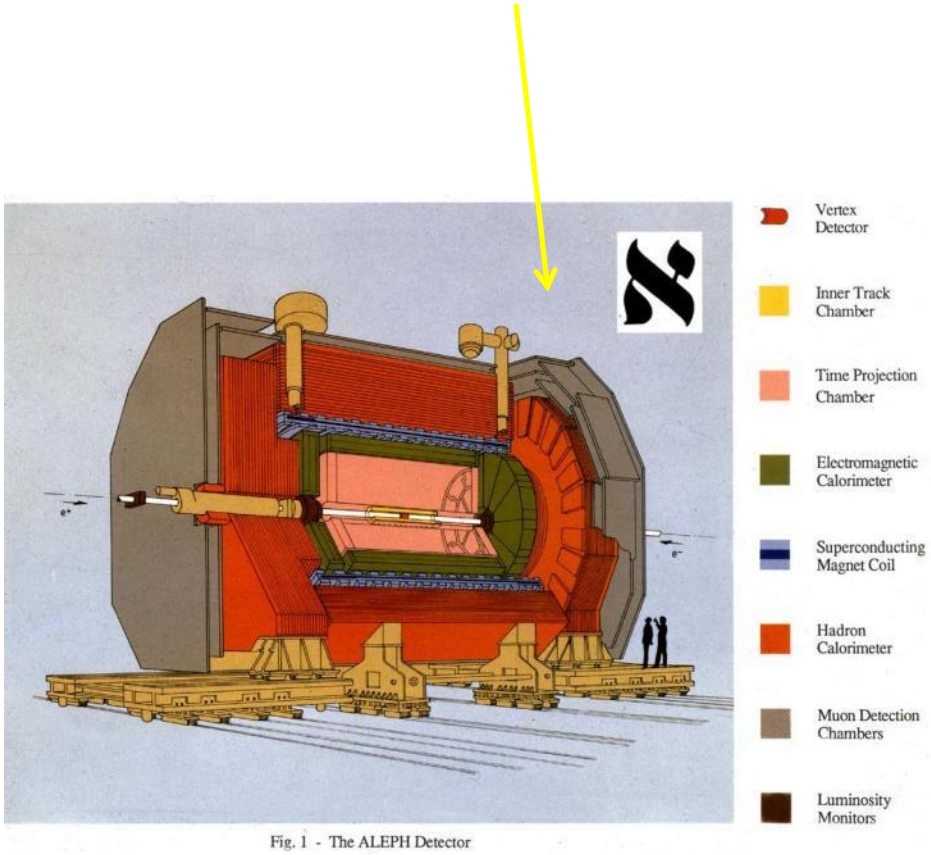

Fig. 1 - The ALEPH Detector

Hadron Calorimeters are large and heavy because the hadronic interaction length λ, the 'strong interaction equivalent' to the EM radiation length X_0, is large (5-10 times larger than X_0)

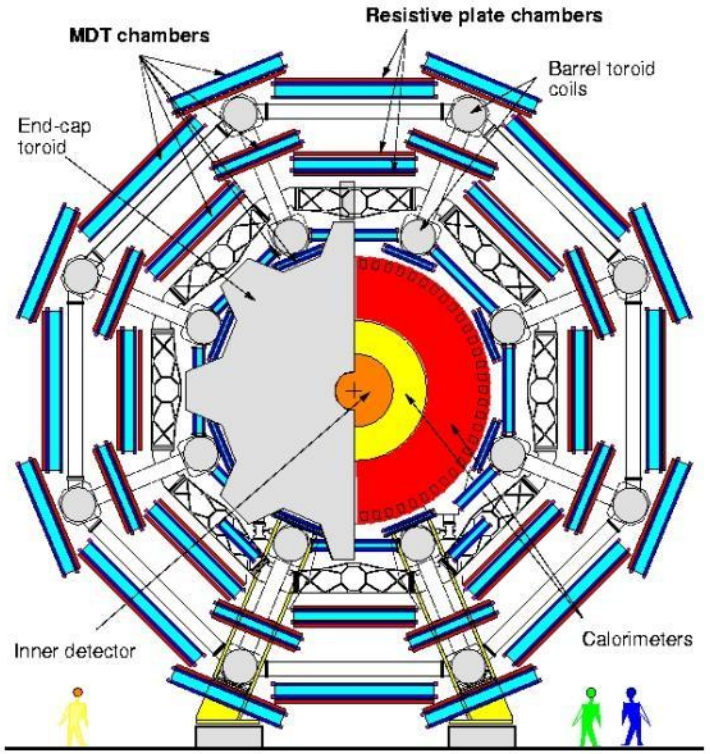

Hadron Calorimeters

By analogy with EM showers, the energy degradation of hadrons proceeds through an increasing number of (mostly) strong interactions with the calorimeter material.

However the complexity of the hadronic and nuclear processes produces a multitude of effects that determine the functioning and the performance of practical instruments, and make hadronic calorimeters more complicated instruments to optimize.

By analogy with EM showers, the energy degradation of hadrons proceeds through an increasing number of (mostly) strong interactions with the calorimeter material.

The hadronic interaction produces two classes of effects:

First, energetic secondary hadrons are produced with a mean free path of λ between interactions. Their momenta are typically a fair fraction of the primary hadron momentum i.e. at the GeV scale.

Second, in hadronic collisions with the material nuclei, a significant part of the primary energy is consumed in nuclear processes such as excitation, nucleon evaporation, spallation etc., resulting in particles with characteristic nuclear energies on the MeV scale.

C.W. Fabjan and F. Gianotti, Rev. Mod. Phys., Vol. 75, N0. 4, October 2003

Because part of the energy is therefore 'invisible', the resolution of hadron calorimeters is typically worse than in EM calorimeters 20-100%/Sqrt[E(GeV)] .

Hadron Calorimeters

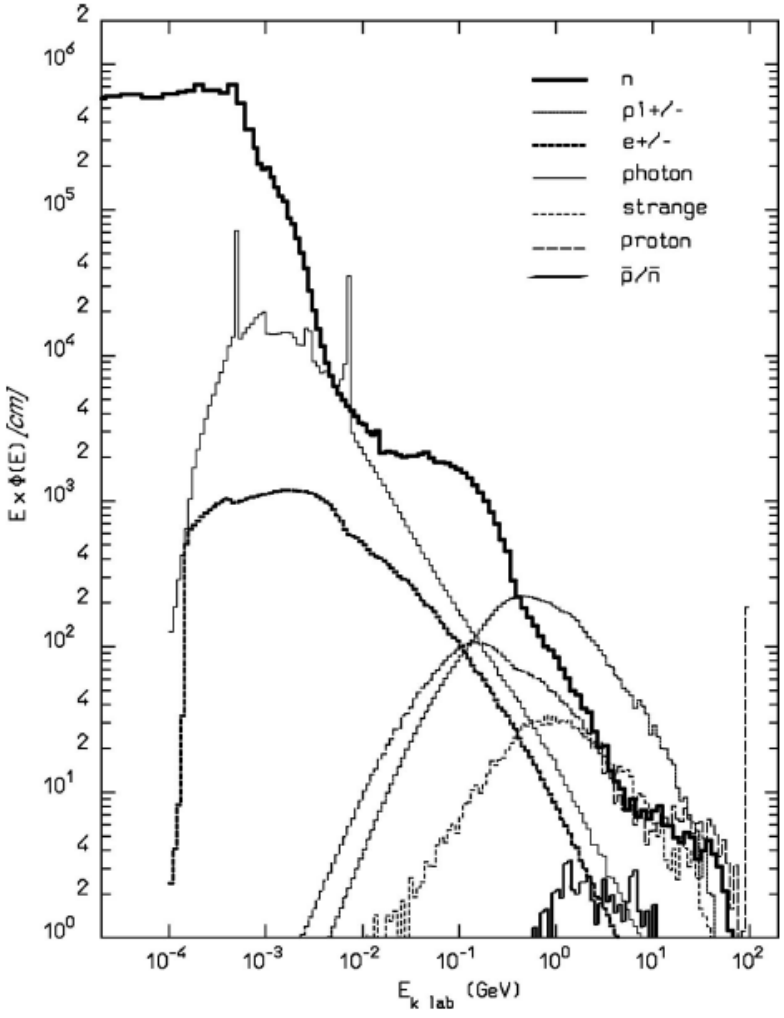

'Deciphering this message becomes the story of hadronic calorimetry'

C.W. Fabjan and F. Gianotti, Rev. Mod. Phys., Vol. 75, N0. 4, October 2003

FIG. 19. Particle spectra produced in the hadronic cascade initiated by 100-GeV protons absorbed in lead. The energetic component is dominated by pions, whereas the soft spectrum is composed of photons and neutrons. The ordinate is in "lethargic" units and represents the particle track length, differential in $\log E$. The integral of each curve gives the relative fluence of the particle. Fluka calculations (Ferrari, 2001).

Hadron Calorimeters

The signals from an electron or photon entering a hadronic calorimeter is typically larger than the signal from a hadron cascade because the hadroic interactions produce a fair fraction of invisible effects (excitations, neutrons …).

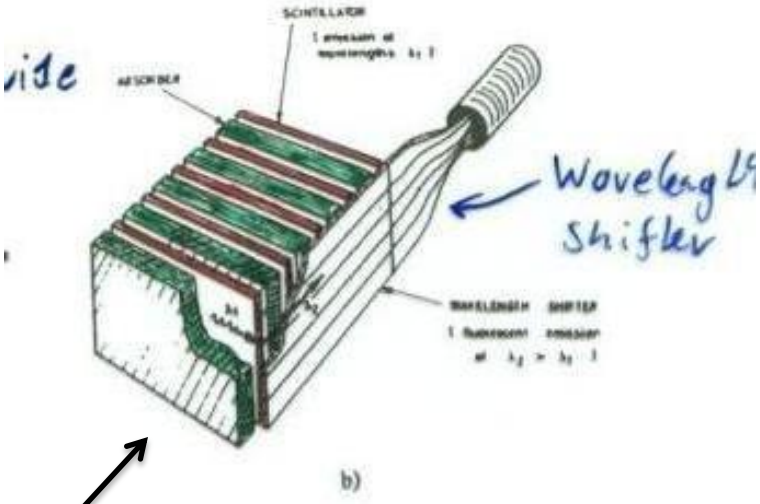

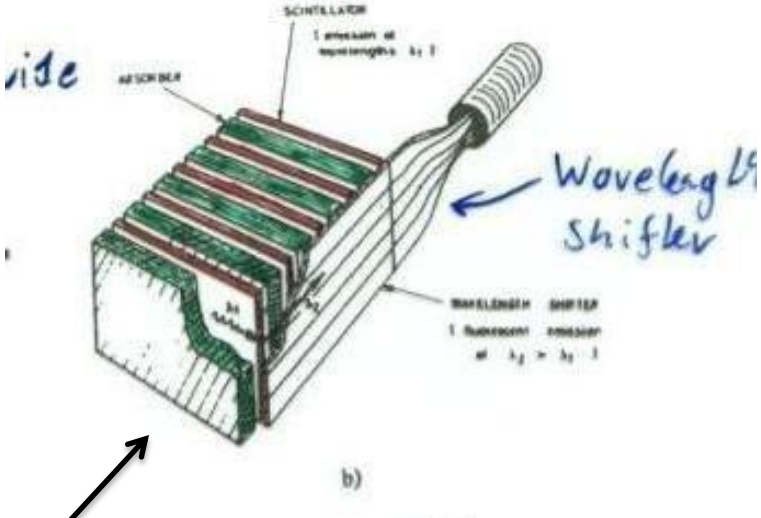

Pion 10GeV

Electron 10GeV

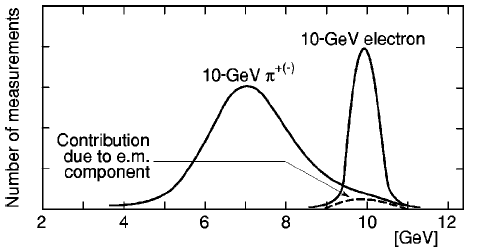

Signal (in energy units) obtained for a 10 GeV energy deposit

Hadron Calorimeters

Because a fair fraction of shower particles consists of π_0 which instantly decay into two photons, part of the hadronic cascade becomes an EM cascade – 'and never comes back'.

Because the EM cascade had a larger response than the Hardon cascade, the event/event fluctuation of produced π_0 particles causes a strong degradation of the resolution.

Is it possible to build a calorimeter that has the same response (signal) for a 10GeV electron and 10GeV hadron ? → compensating calorimeters.

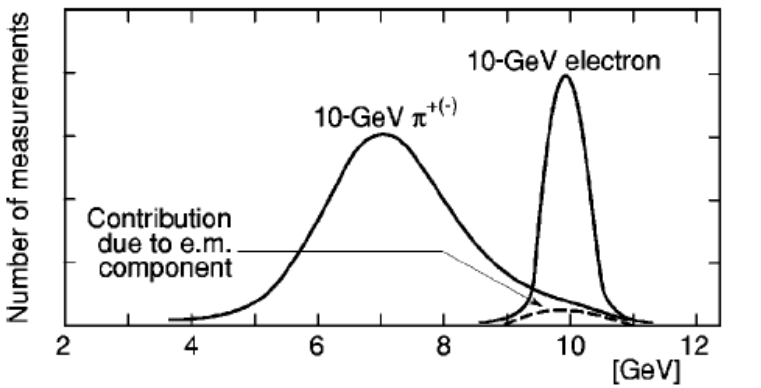

Signal (in energy units) obtained for a 10 GeV energy deposit

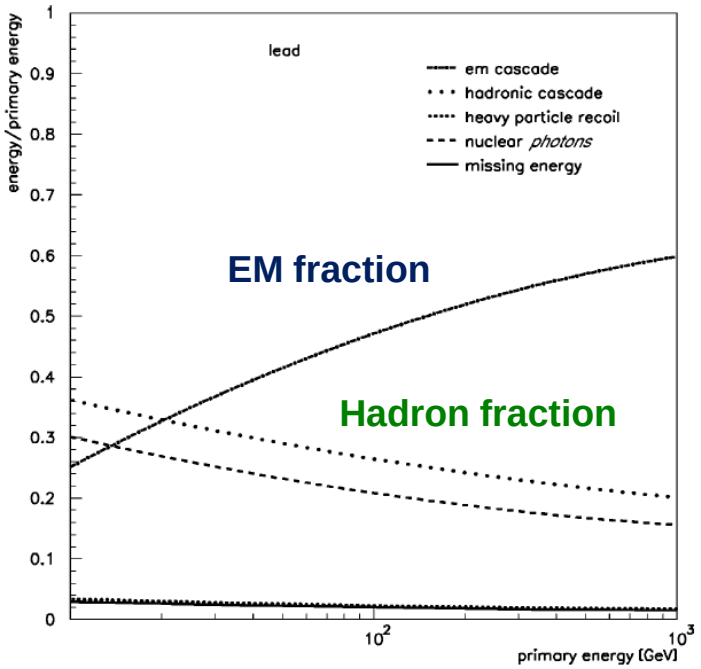

FIG. 21. Characteristic components of proton-initiated cascades in lead. With increasing primary energy the π^0 component increases (Ferrari, 2001).

Compensating Hadron Calorimeters

In a homogeneous calorimeter it is clearly not possible to have the same response for electrons and hadrons.

For sampling calorimeters the sampling frequency and thickness of active and possibe layers can be tunes such that the signal for electrons and hadrons is indeed equal !

Using Uranium or Lead with scintillators, hadron calorimters with excellen energy resolution and linearity have been built.

Energy resolution

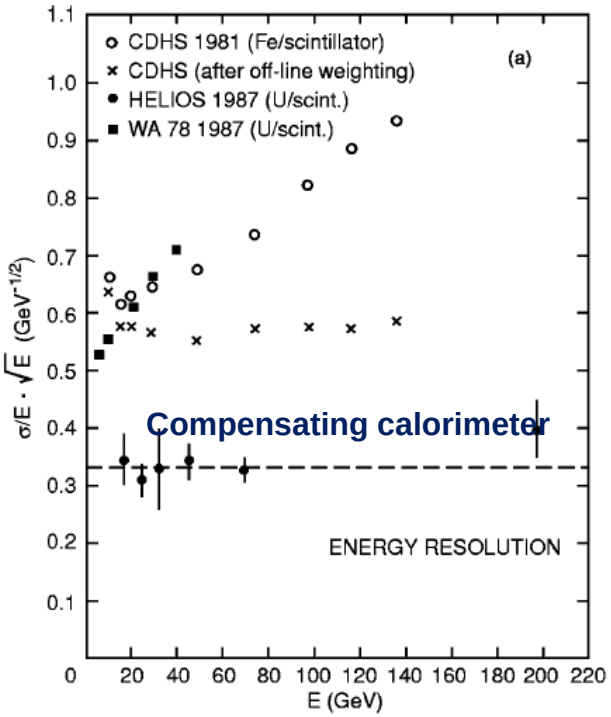

Linearity

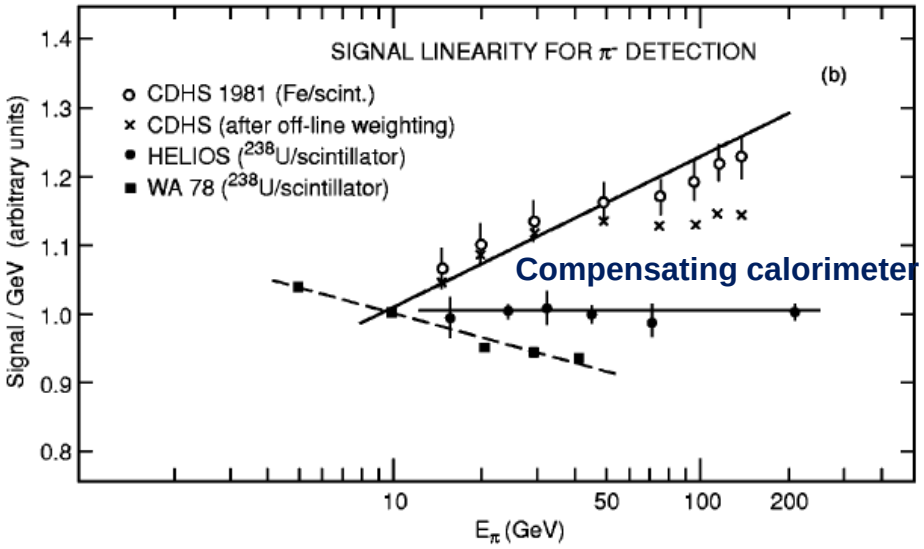

Compensating Hadron Calorimeters

Resolution and linearity of a hadron calorimeter is best if e/h=1. For all other values e/h<>1 the resolution in linearity is worse.

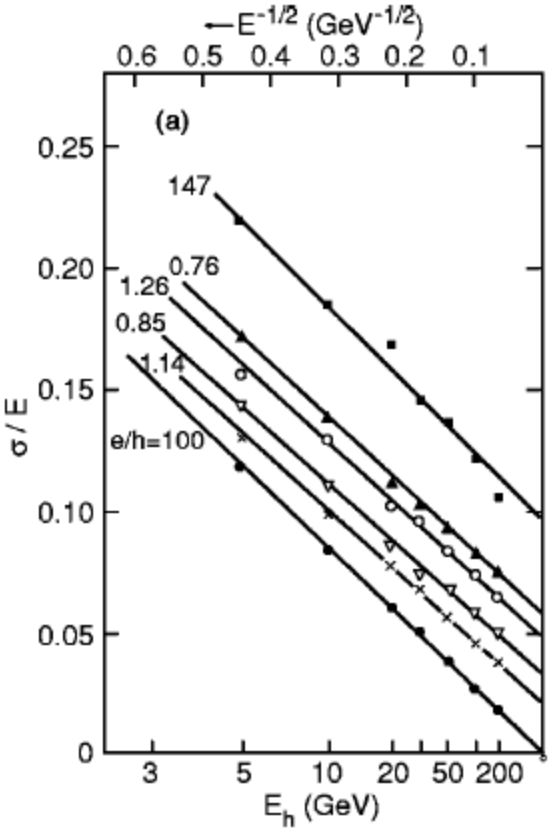

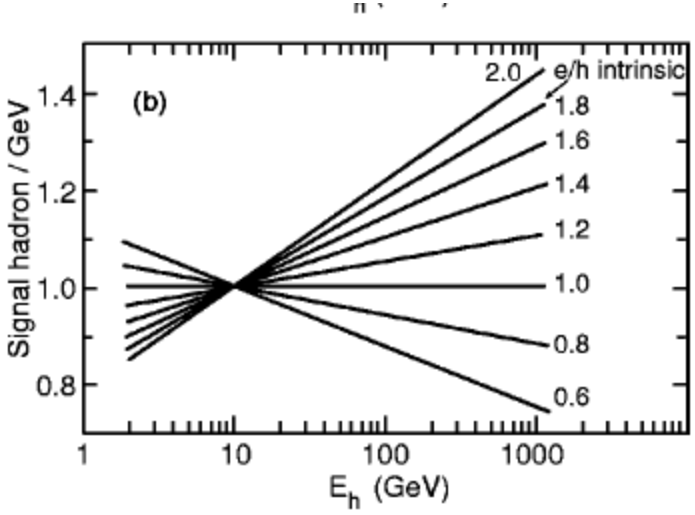

FIG. 24. Monte Carlo simulation of the effects of $e/\pi \neq 1$ on energy resolution (a) and response linearity (b) of hadron calorimeters with various values for e/h (intrinsic), where h (intrinsic) denotes the response to the purely hadronic component of the shower (Wigmans, 1988).

Particle ID

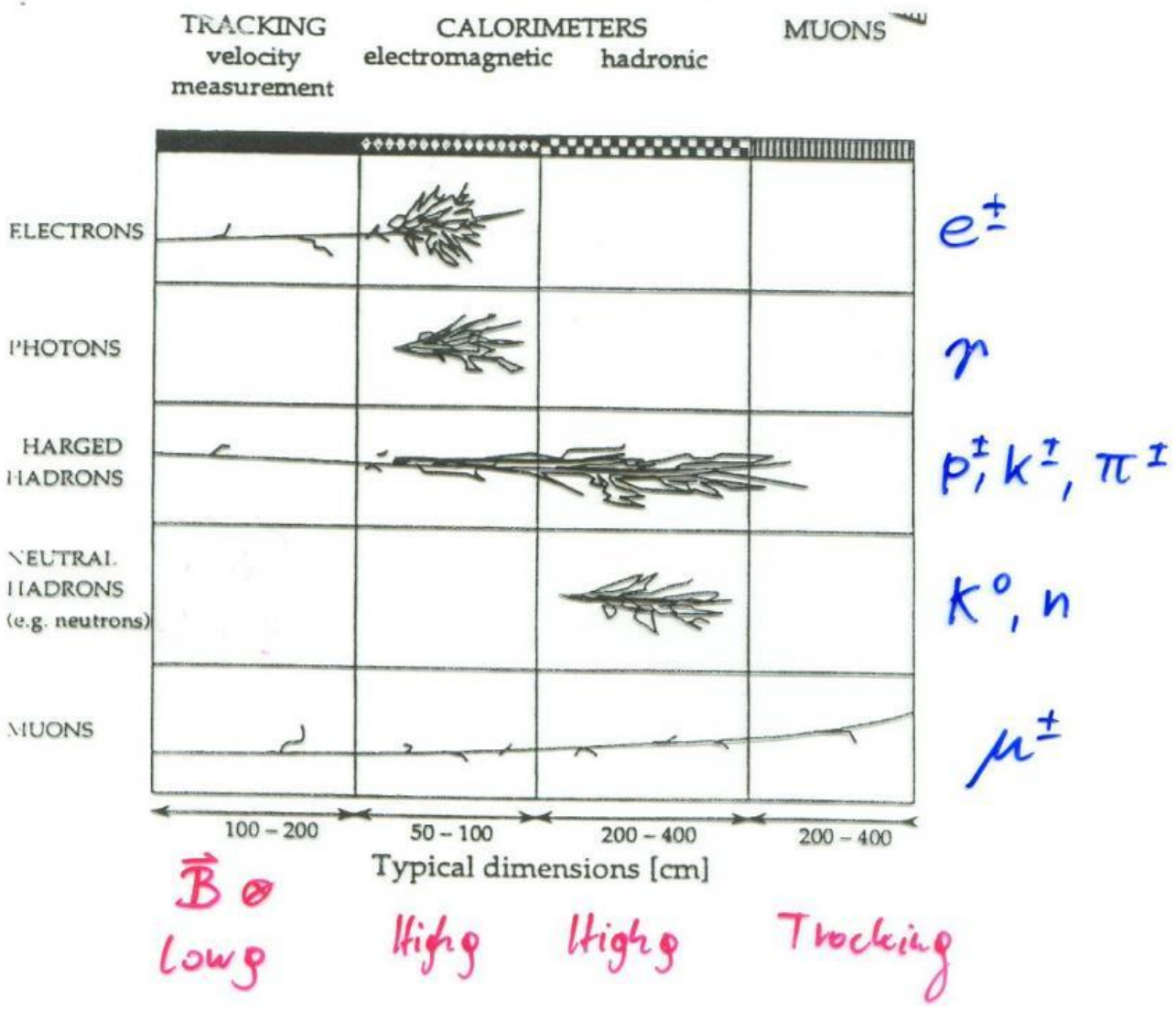
TRACKING
velocity measurement
CALORIMETERS
electromagnetic
hadronic
MUONS
ELECTRONS
PHOTONS
HARGED HADRONS
NEUTRAL HADRONS (e.g. neutrons)
MUONS
100 – 200
50 – 100
200 – 400
200 – 400
Typical dimensions [cm]
$e^{\pm}$
γ
$p^{\pm}, k^{\pm}, \pi^{\pm}$
K^0, n
$\mu^{\pm}$
$\vec{B}$ ⊗
Low p
High p
High p
Tracking

Particle Identification

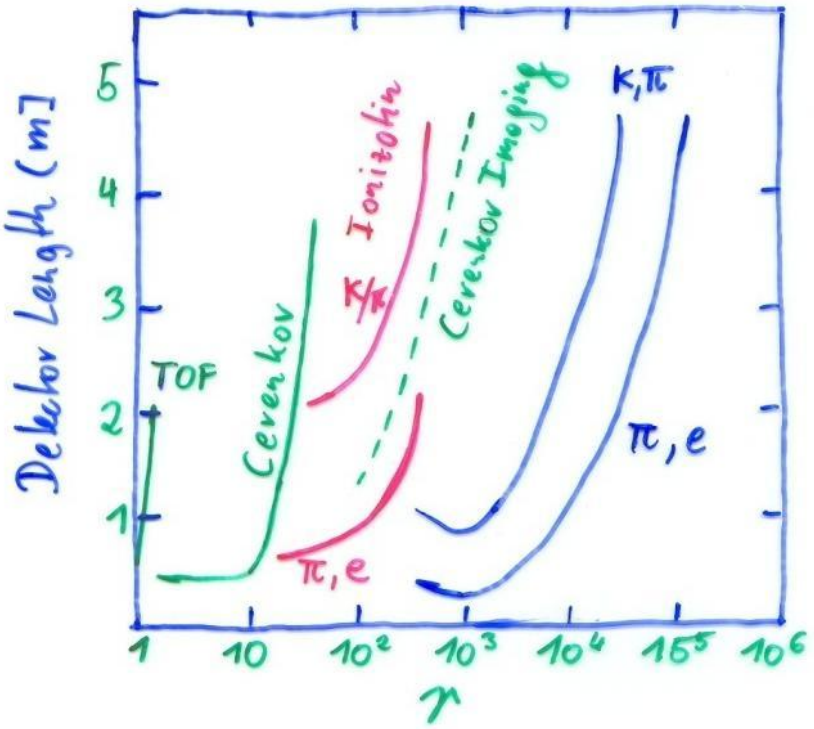

1) • For low Energies the Time of Flight (TOF) measures the velocity $p, v \rightarrow m$

2) • For longer Energies the Cerenkov Threshold $v > \frac{c}{n}$ discriminates between Particles

3) • For $\gamma \sim 100$ the multiple $\frac{dE}{dx}$ measurements provide Identification

4) • Cerenkov Angle Measurements $\cos\theta = \frac{1}{n\beta}$ provide Particle ID

5) • At very high γ the Transition Radiation allows Identification

dE/dx

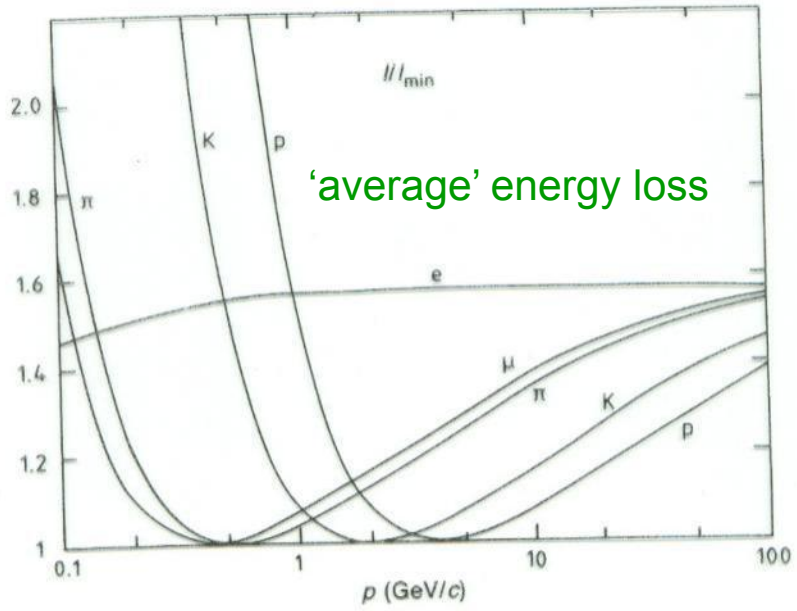

‘average’ energy loss

Measured energy loss

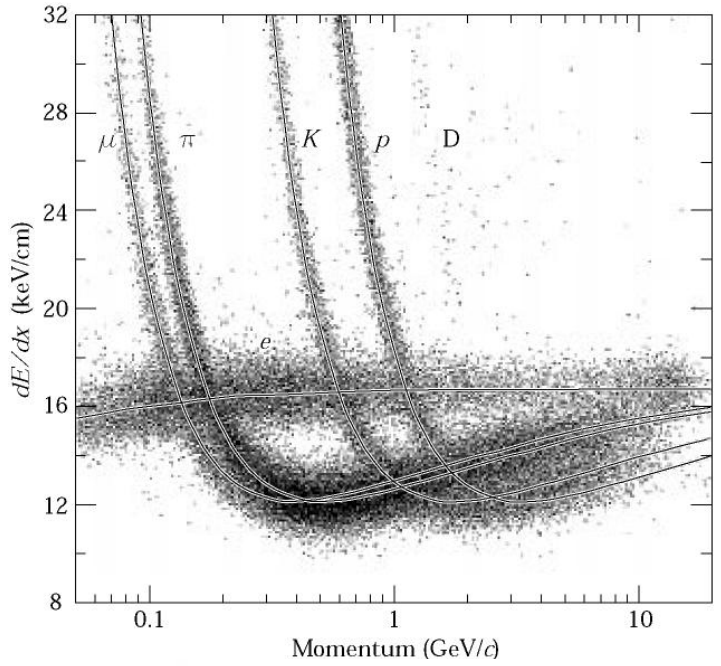

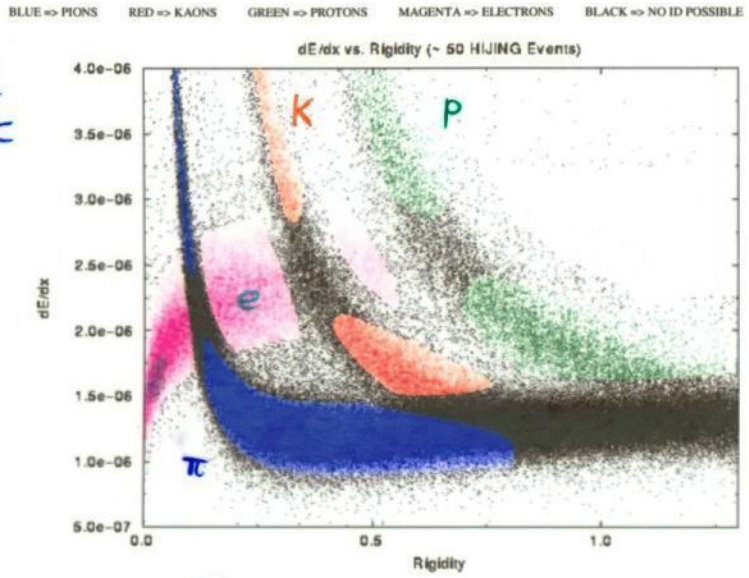

In certain momentum ranges, particles can be identified by measuring the energy loss.

Time of Flight (TOF)

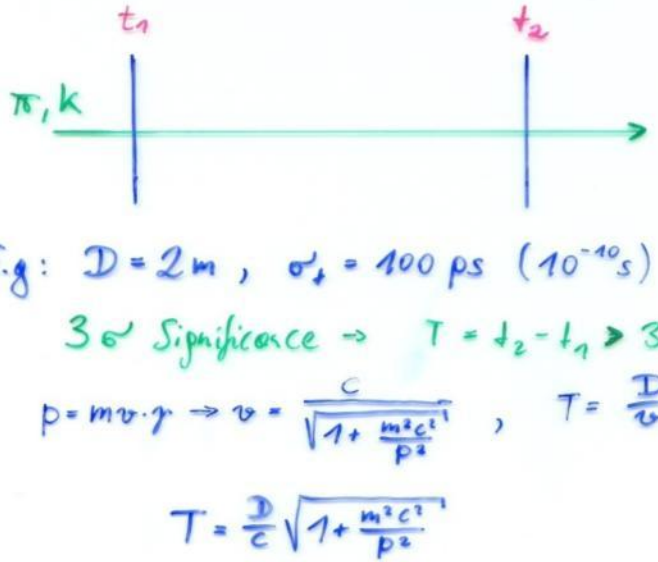

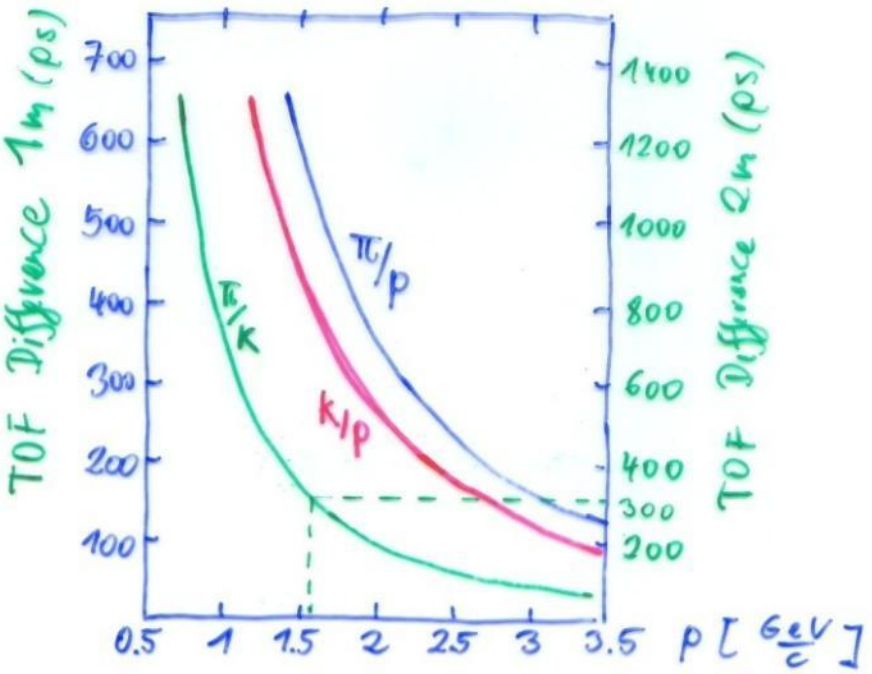

NA49 combined particle ID: TOF + dE/dx (TPC)

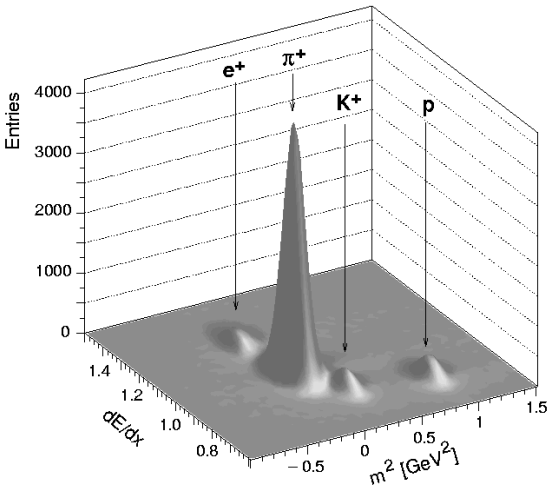

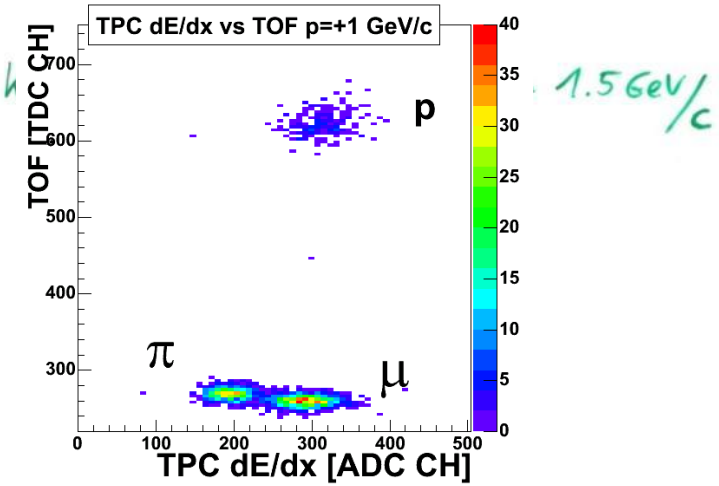

Cherenkov Radiation

If the velocity of a charged particle is larger than the velocity of light in the medium $v > \frac{c}{n}$ (n ... Refractive Index of Material) it emits 'Cherenkov' radiation at a characteristic angle of $\cos\theta_c = \frac{1}{n\beta}$ $(\beta = \frac{v}{c})$

$$\frac{dN}{dx} \sim 2\pi\alpha z_1^2 \left(1 - \frac{1}{\beta^2 n^2}\right) \frac{\lambda_2 - \lambda_1}{\lambda_2 \cdot \lambda_1}$$

= Number of emitted Photons / length with λ between λ_1 and λ_2

With $\lambda_1 = 400\,nm$ $\lambda_2 = 700\,nm$

$$\frac{dN}{dx} = 490 \left(1 - \frac{1}{\beta^2 n^2}\right) \left[\frac{1}{cm}\right]$$

Material	$n-1$	β threshold	γ threshold
solid Sodium	3.22	0.24	1.029
lead glass	0.67	0.60	1.25
water	0.33	0.75	1.52
silica aerogel	0.025-0.075	0.93-0.976	2.7 - 4.6
air	$2.93 \cdot 10^{-4}$	0.9997	41.2
He	$3.3 \cdot 10^{-5}$	0.99997	123

Ring Imaging Cherenkov Detector

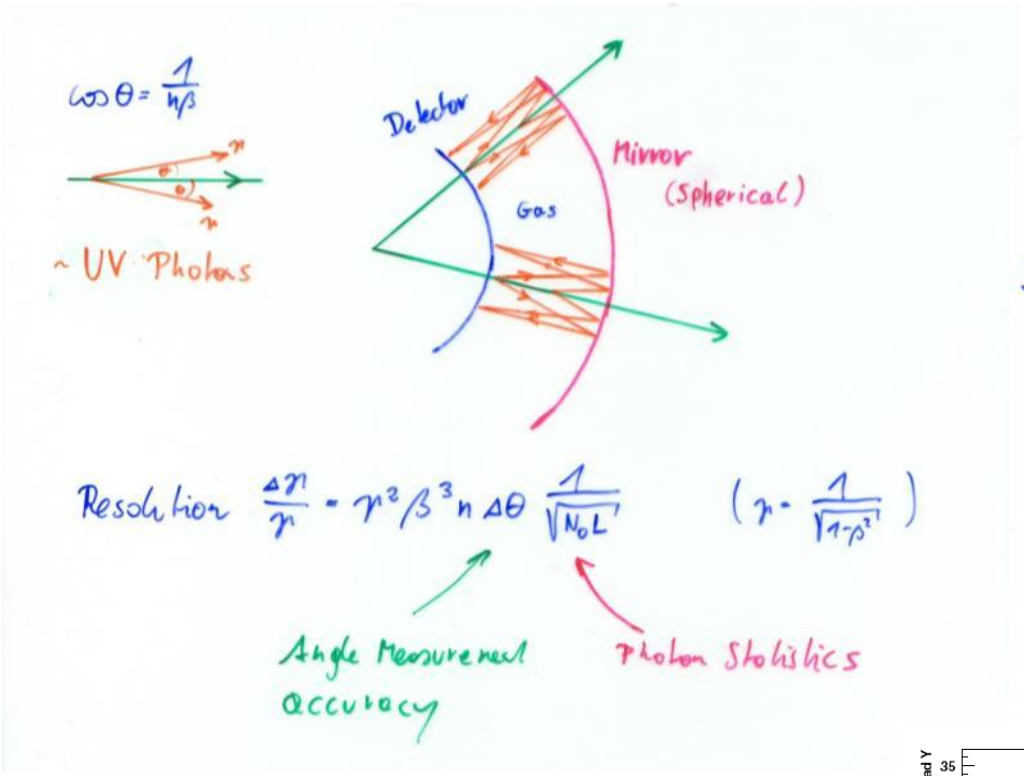

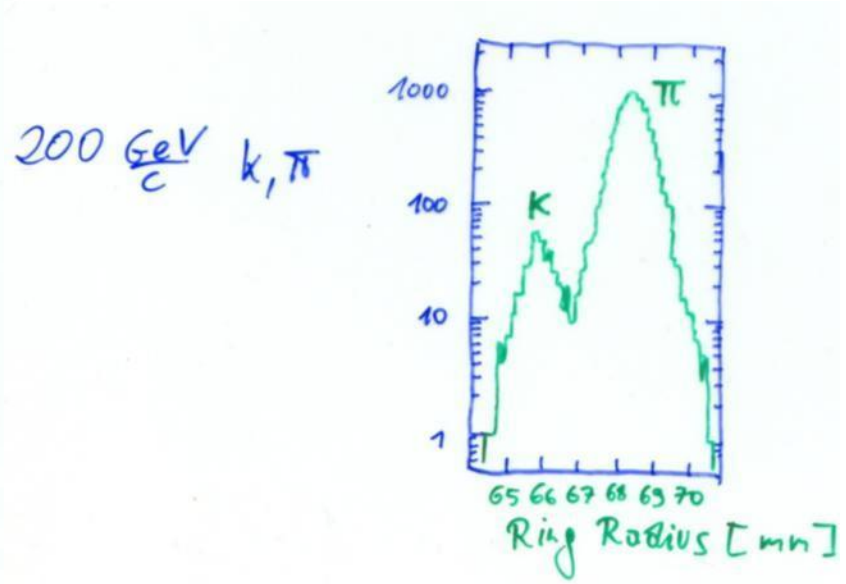

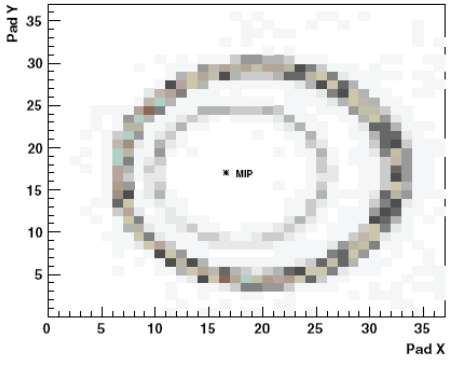

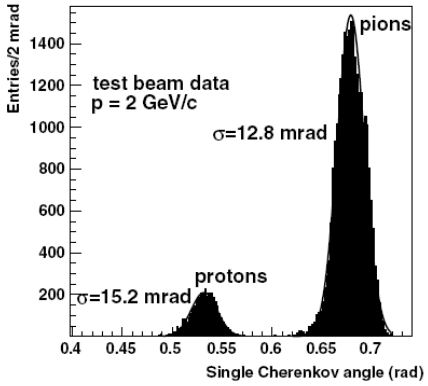

Transition Radiation

Radiation (~ keV) emitted by
ultra-relativistic Particles when they
traverse the boarder of 2 Materials
of different Dielectric Permittivity ($\varepsilon_1, \varepsilon_2$)

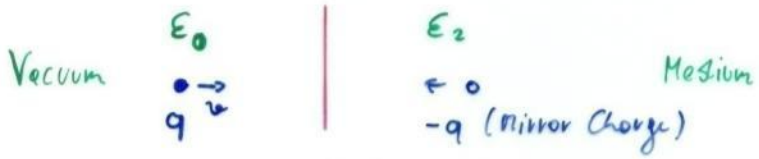

Classical Picture

$q = z_1 e$

$I = \frac{1}{3} \alpha z_1^2 (\hbar\omega_p) \gamma$ ... Radiated Energy per Transition

$\hbar\omega_p$ .... plasma Frequency of the Medium
.... ~20 eV for Styrene

About half the Energy is radiated between

$0.1 \hbar\omega_p \gamma < \hbar\omega < \hbar\omega_p \gamma$

E.g. $\gamma = 1000$ 2-20 keV X-Rays

$N_\gamma \sim \frac{2}{3} \alpha z_1^2 \sim 5 \cdot 10^{-3} \cdot z_1^2$

γ-Dependence from hardening rather than N_γ

Emission Angle ~ $\frac{1}{\gamma}$

The Number of Photons can be increased by
placing many foils of Material.

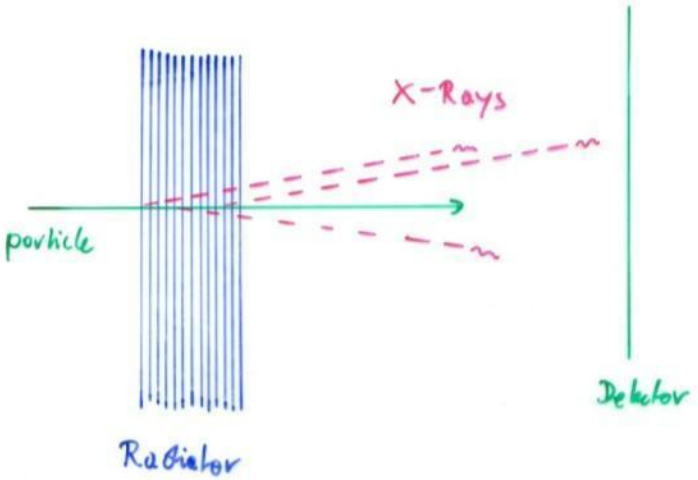

Instrumenting the Earth's Atmosphere or the Polar Ice Cap we get huge Calorimeters for Astro Particle Physics !

Examples:

AMANDA on the South Pole

Pierre Auger Telescope in South America

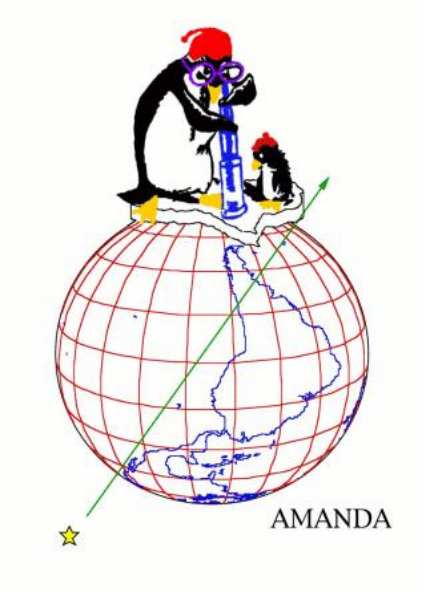

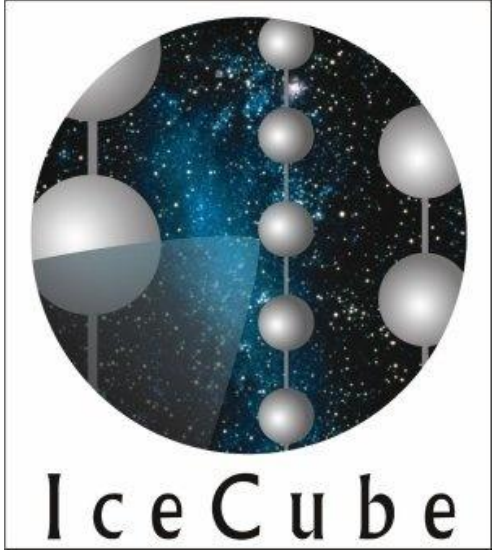

AMANDA

Antarctic **M**uon **A**nd **N**eutrino **D**etector **A**rray

AMANDA

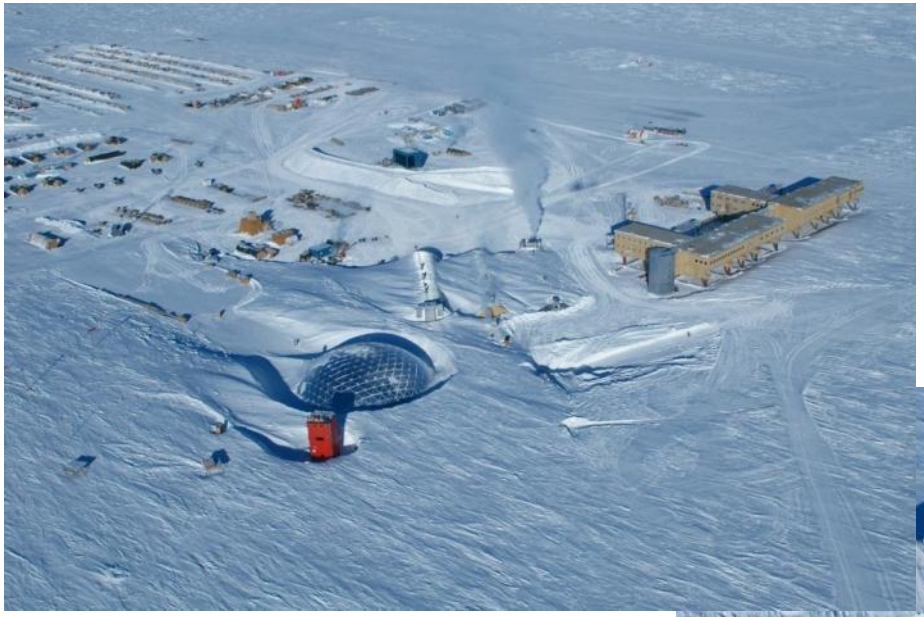

South Pole

AMANDA

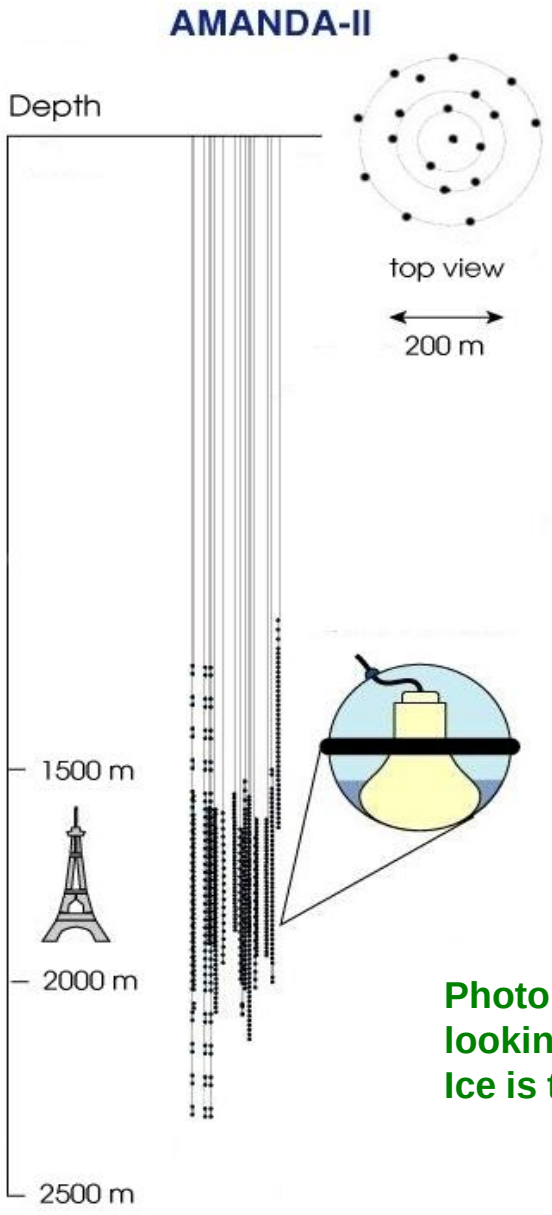

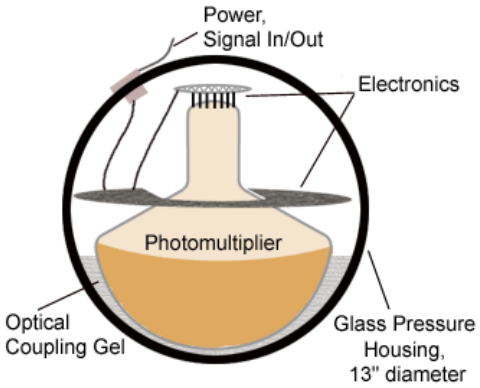

Photomultipliers in the Ice,
looking downwards.
Ice is the detecting medium.

AMANDA

Look for upwards going Muons from Neutrino Interactions.
Cherekov light propagating through the ice.

→ Find neutrino point sources in the universe !

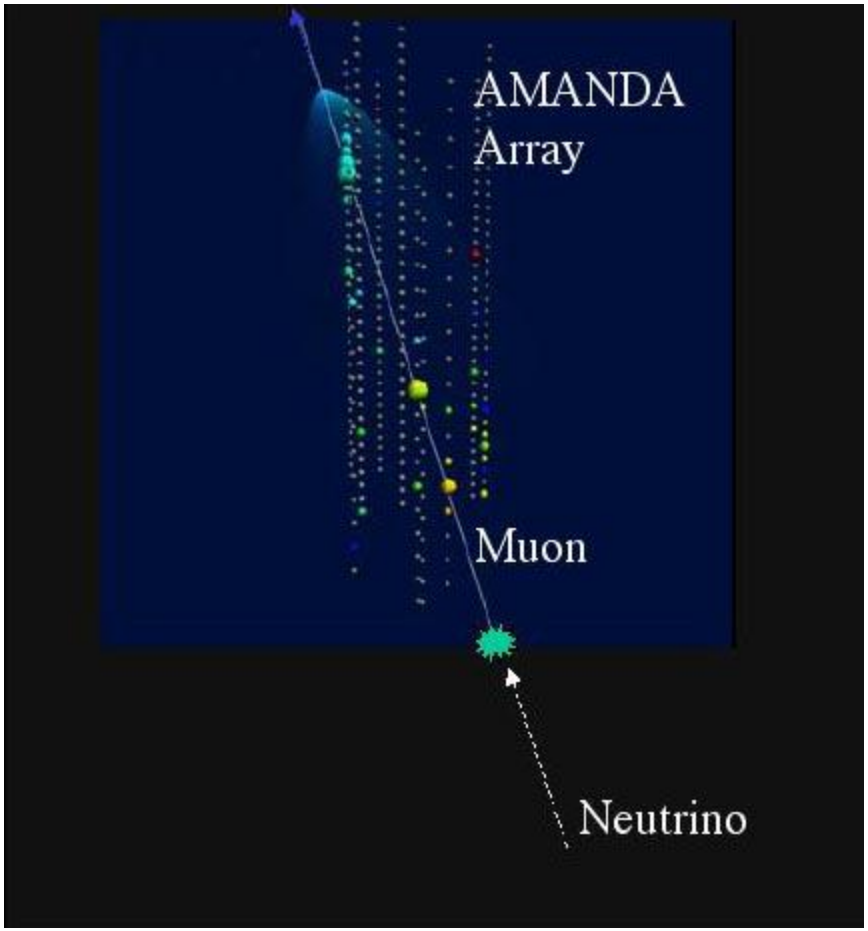

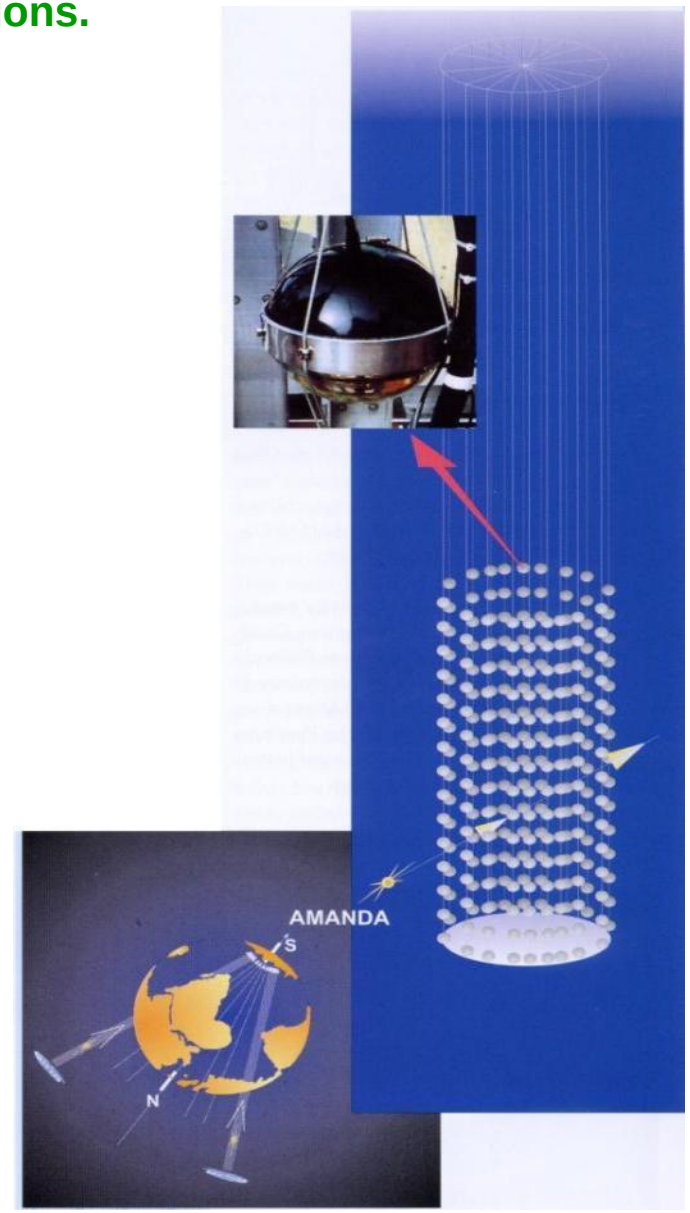

AMANDA

Event Display

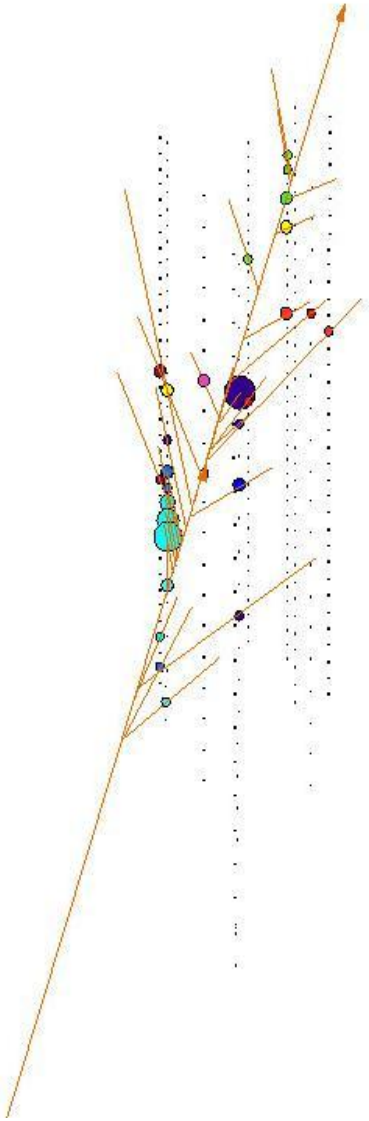

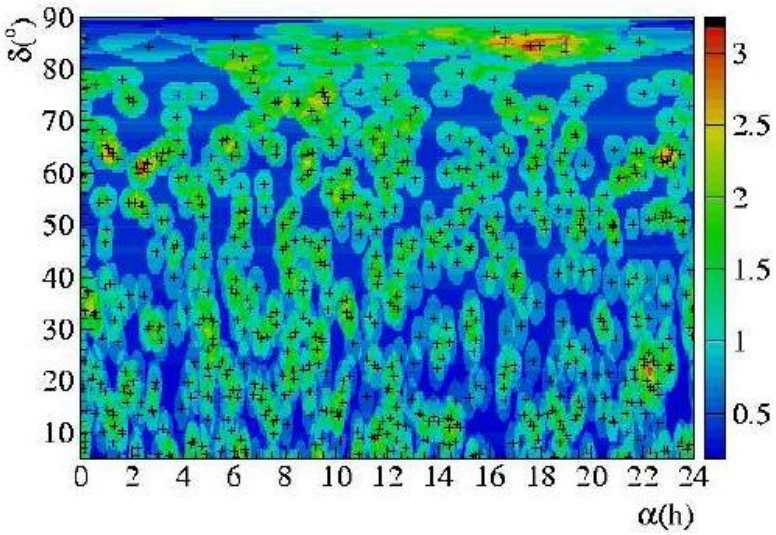

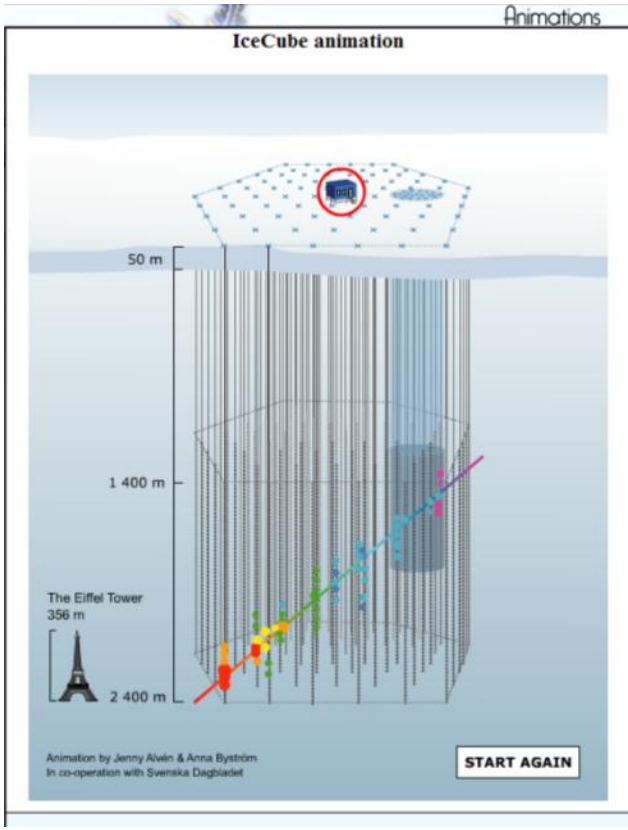

Up to now: No significant point sources but just neutrinos from cosmic ray interactions in the atmosphere were found .

→ Ice Cube for more statistics !

Pierre Auger Cosmic Ray Observatory

Pierre Auger Cosmic Ray Observatory

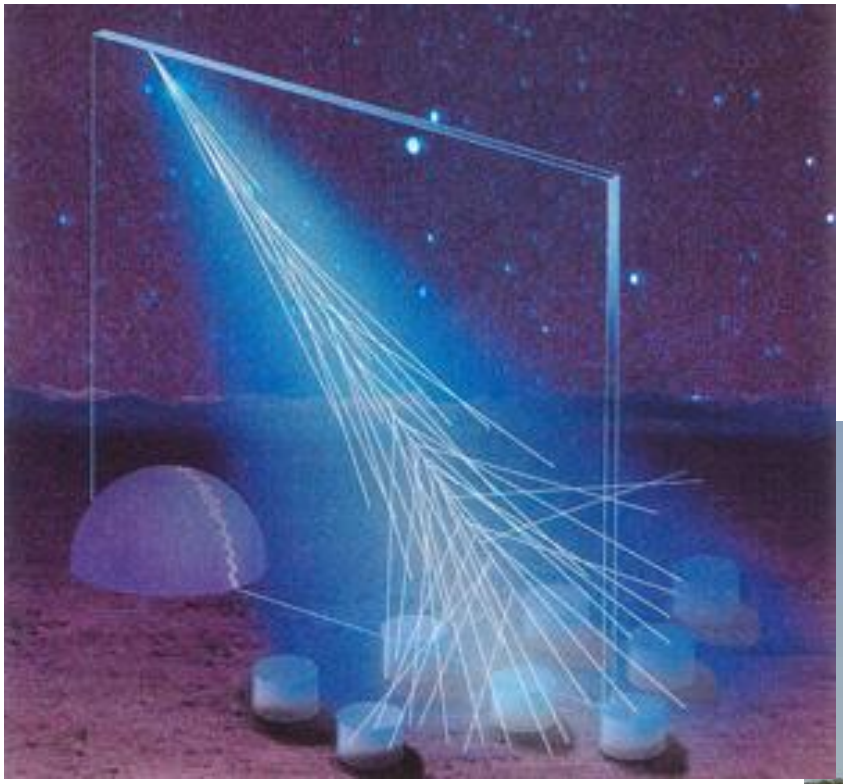

Use earth's atmosphere as a calorimeter. 1600 water Cherenkov detectors with 1.5km distance.

Placed in the Pampa Amarilla in western Argentina.

Pierre Auger Cosmic Ray Observatory

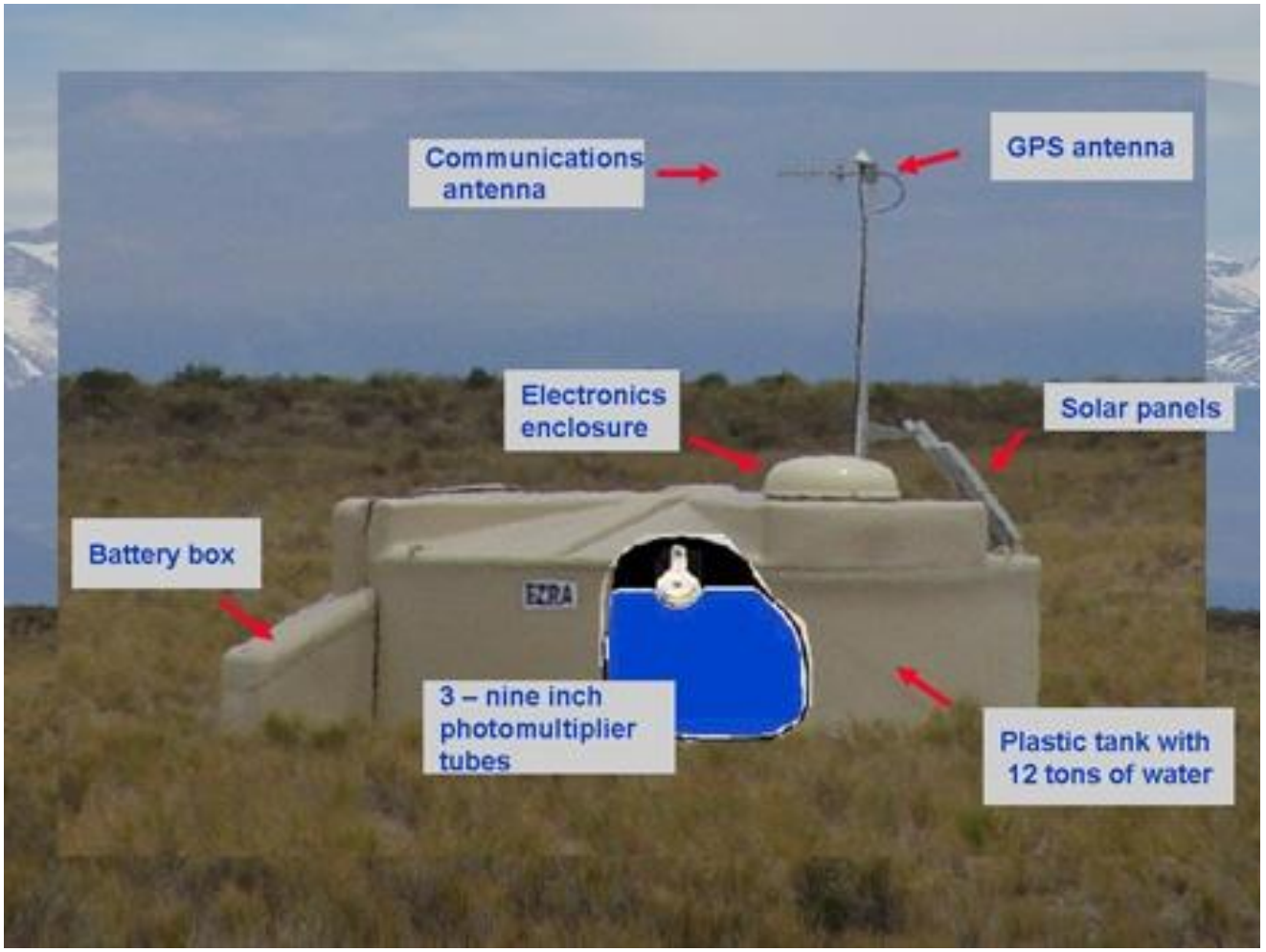

Pierre Auger Cosmic Ray Observatory

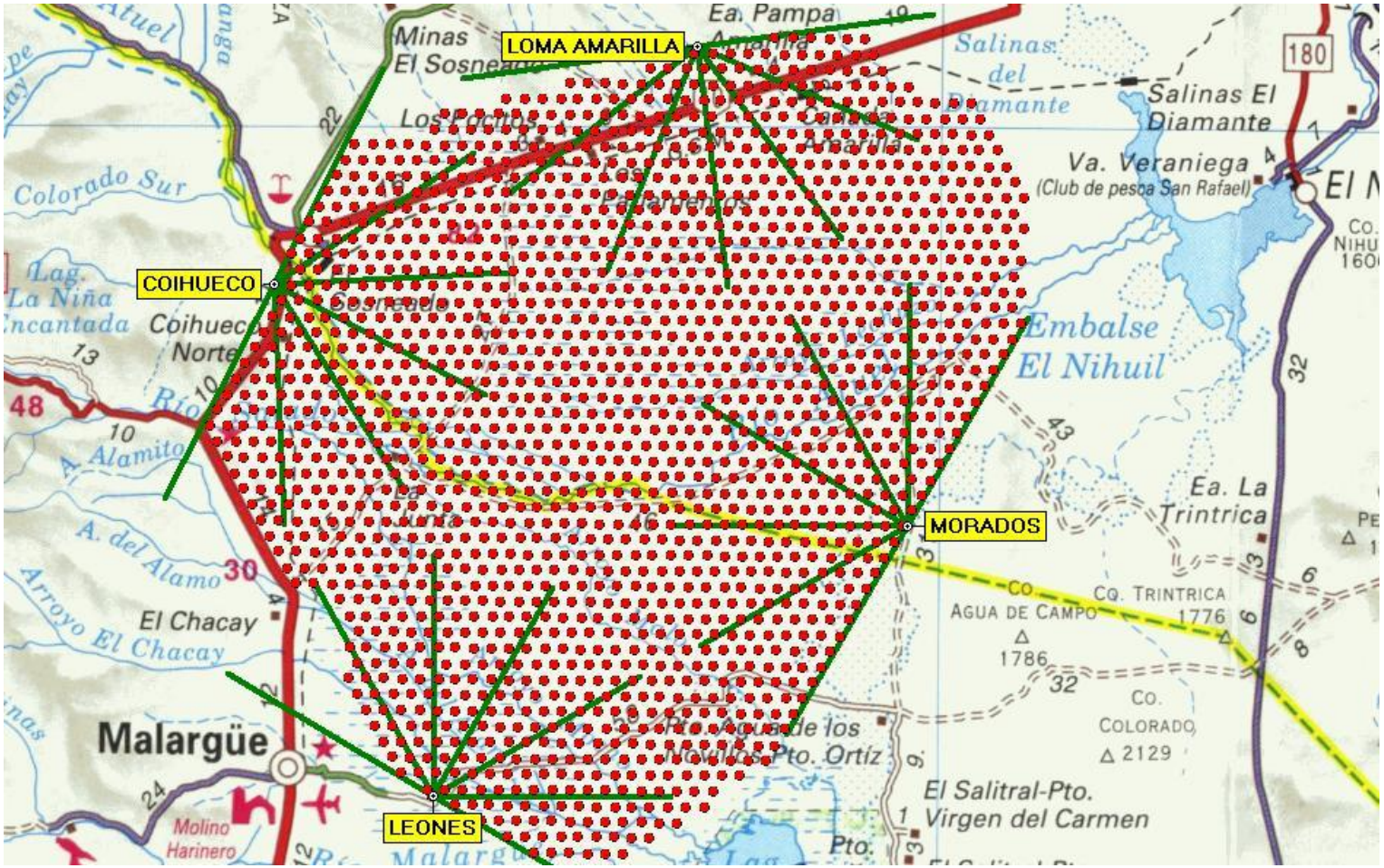

Pierre Auger Cosmic Ray Observatory

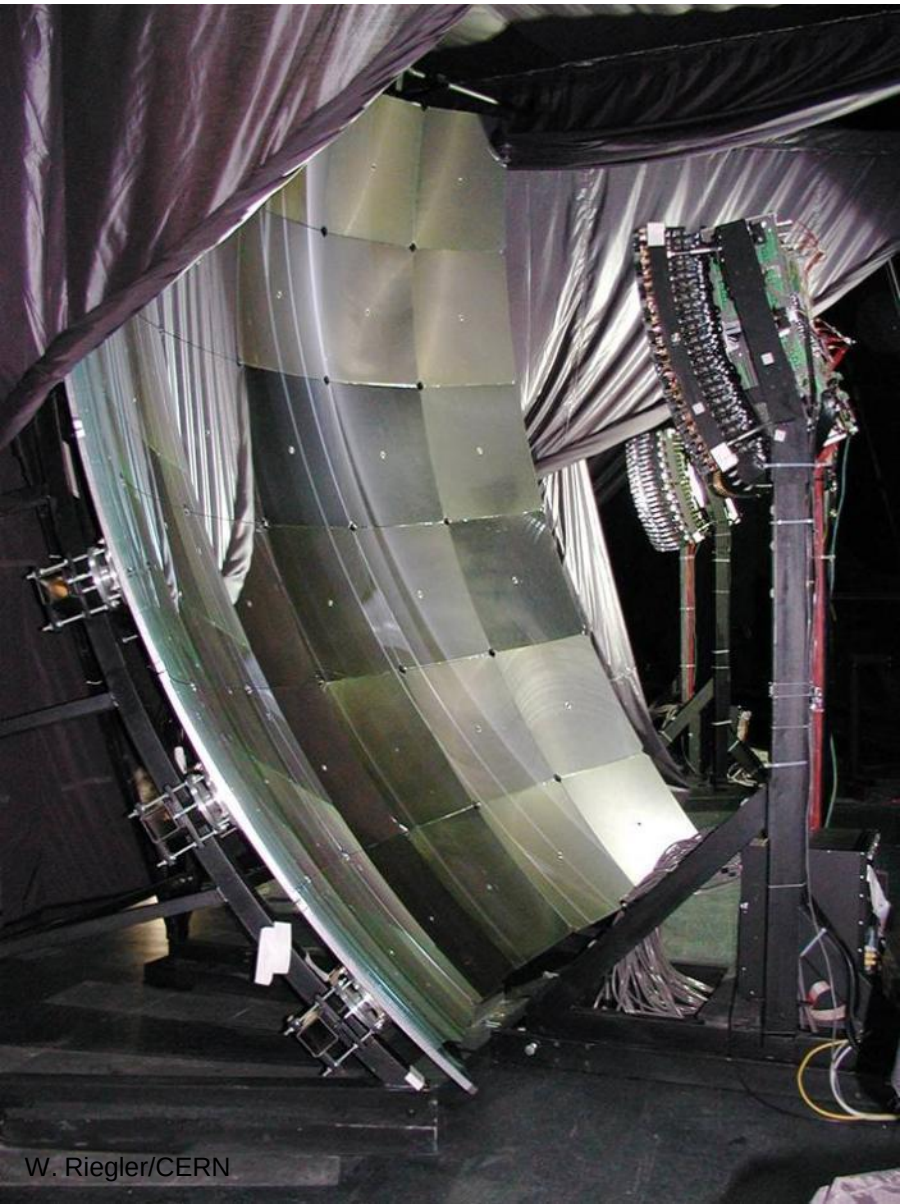

W. Riegler/CERN

In addition: Fluorescence detectors around the array of water tanks.

Event 1234800

See CR incoming direction | See individual station data

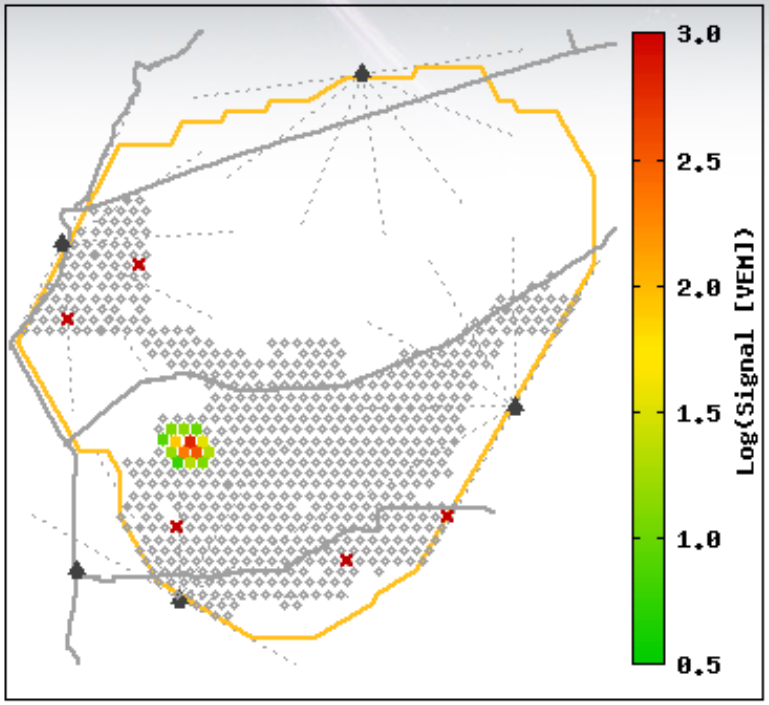

37 EeV = Exa Electron Volt = 37 x 10^{18} eV

Generic Information	
Id	1234800
Date	Sat Mar 5 15:54:48 2005
Nb Station	14
Energy	37.4 ± 1.2 EeV
Theta	43.4 ± 0.1 deg
Phi	-27.3 ± 0.2 deg
Curvature	15.8 ± 0.8 km
Core Easting	460206 ± 20 m
Core Northing	6089924 ± 11 m
Reduced Chi^2	2.30

Event 1234800

See event reconstruction data | See CR incoming direction

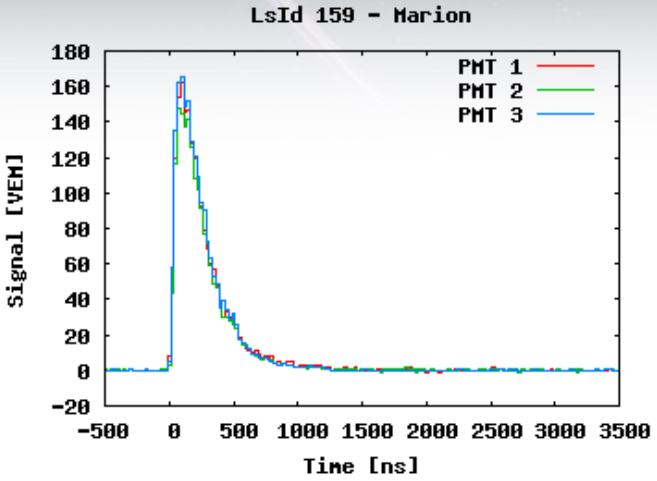

Signal in VEM for the 3 PMTs of station 159 (Marion) as a function of time

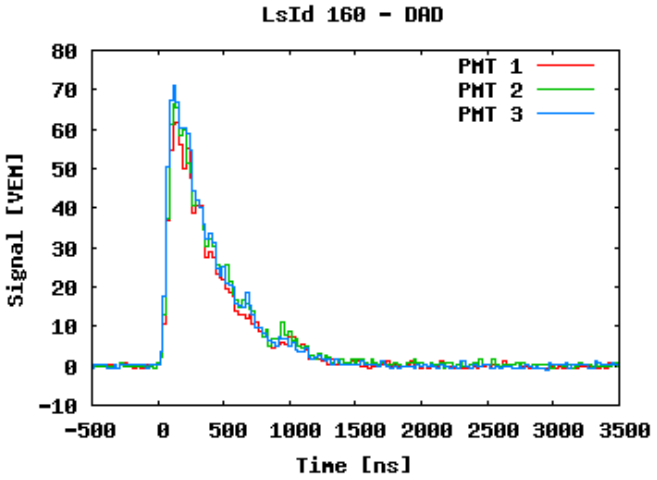

Signal in VEM for the 3 PMTs of station 160 (DAD) as a function of time

Conclusion

The story of modern calorimetry is a textbook example of physics research driving the development of an experimental method.

The long quest for precision electron and photon spectroscopy explains the remarkable progress in new instrumentation techniques, for both sampling and homogeneous calorimeters.

The study of jets of particles as the macroscopic manifestation of quarks has driven the work on hadronic calorimeters.

C.W. Fabjan and F. Gianotti, Rev. Mod. Phys., Vol. 75, N0. 4, October 2003